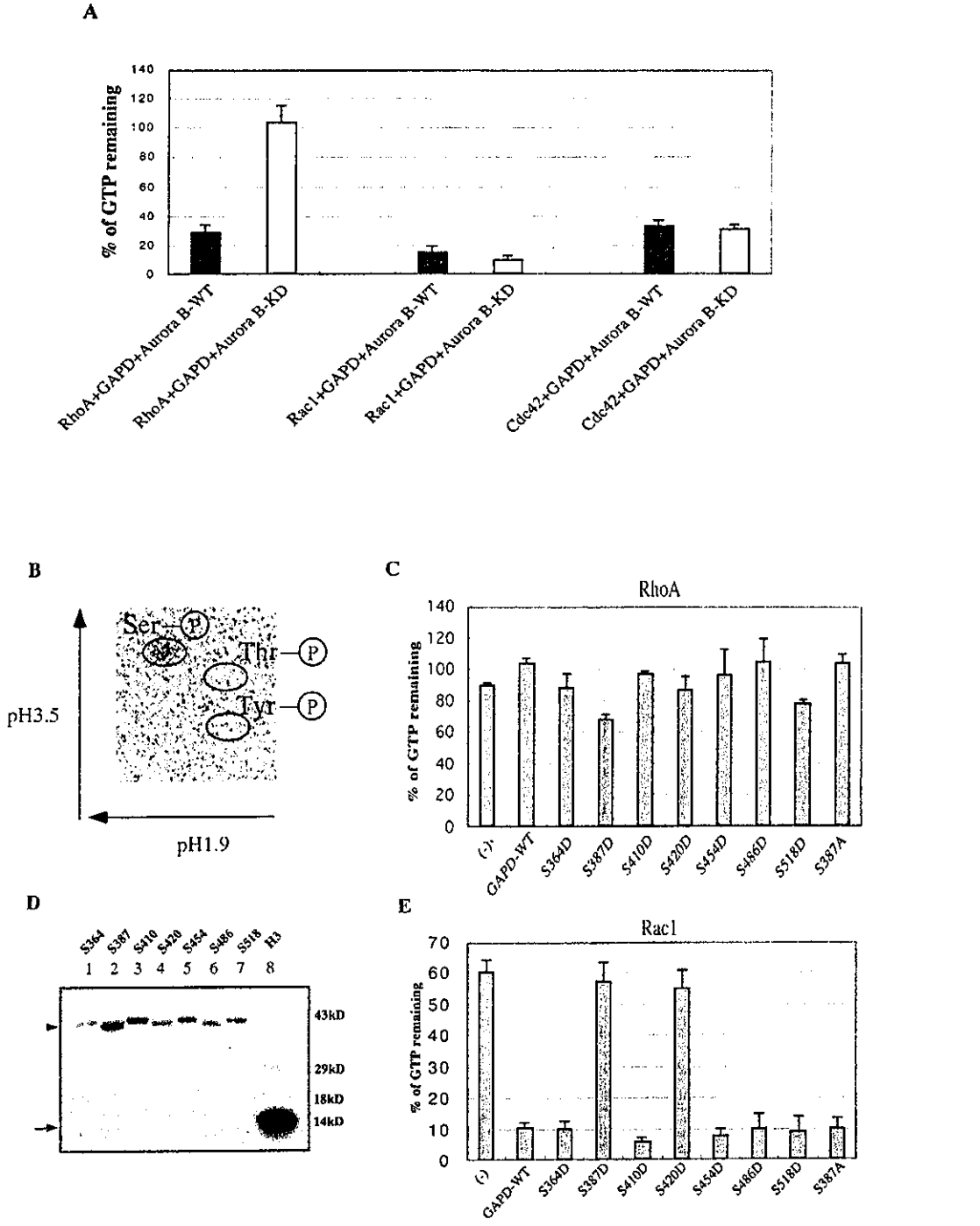

Figure 4. Phosphorylation of MgcRacGAP by Aurora B Occurs at Ser387, Induces Latent GAP Activity toward RhoA, and Downregulates the GAP Activity toward Rac1 and Cdc42

(A) Phosphorylation of the C terminus *GAP* domain (GAPD) of MgcRacGAP induced by Aurora B led to induction of latent GAP activity toward RhoA. We did GTP hydrolysis assays and measured GAP activities of the purified GAPD, with or without the phosphorylation induced by Aurora B. The GAPD protein was first incubated with the WT- or KD-Aurora B under conditions similar to those described for Figures 3A and 3C but with some modifications, with a longer incubation (2 hr) and without the use of [γ^{32}P]ATP. We then did the GTP hydrolysis assay toward RhoA, Rac1, and Cdc42 using these reaction mixtures. The results shown are the averages ± the standard deviations (SD) of three independent experiments.

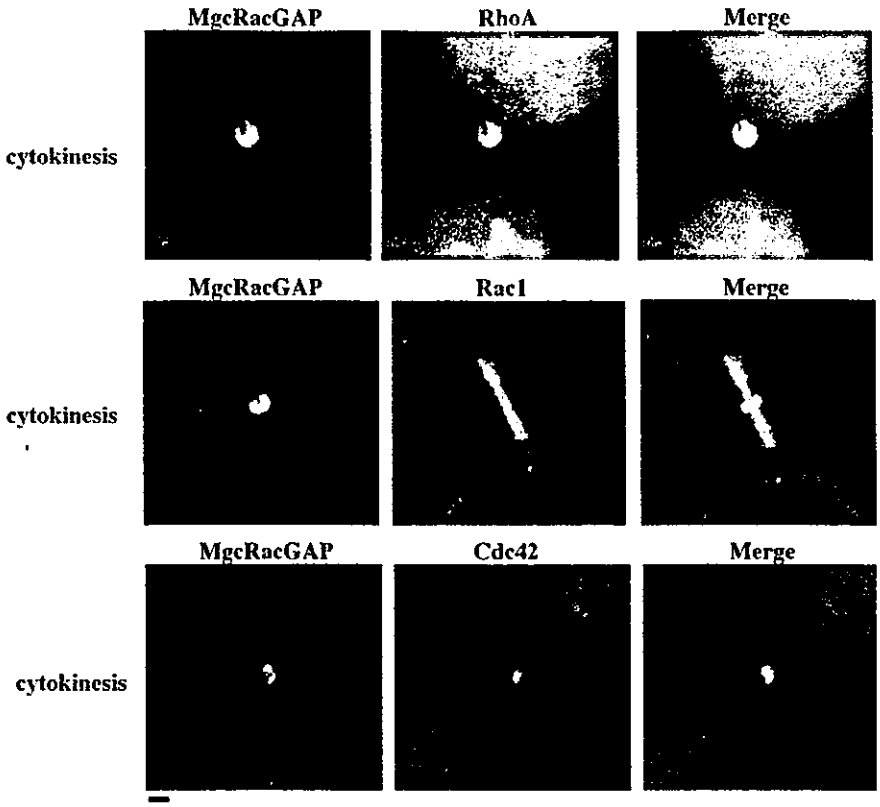

Figure 5. Localization of RhoA, Rac1, Cdc42, and MgcRacGAP during Mitosis

Colocalization of MgcRacGAP with RhoA but not with Rac1 or Cdc42 in the midbody. HeLa cells were fixed and stained with the anti-RhoA mAb (upper panels, red), anti-Rac1 mAb (middle panels, red), anti-Cdc42 mAb (lower panels, red), and anti-MgcRacGAP antibody (all panels, green). The immunostained coverslip was viewed under a confocal microscope. The scale bar represents 2 μm.

and MgcRacGAP are accumulated on the actin-based contractile ring during cytokinesis. Some accumulation of Cdc42 protein was observed at the equator of the central spindle and was encircled by the ring of MgcRacGAP (Figure 5, lower panels). However, it did not colocalize with MgcRacGAP. Taken together, it is strongly suggested that the target small GTPase of MgcRacGAP is RhoA at the late stage of cytokinesis.

Ser387 Is Phosphorylated In Vivo at the Midbody

Ser387 of MgcRacGAP seemed to be an important phosphorylation site that alters its GAP activities on RhoA, Rac1, and Cdc42 in vitro. Therefore, we generated a site- and phosphorylation state-specific rabbit polyclonal antibody for this site (referred to as anti-pS387 Ab), using the synthetic phosphopeptide PM387 (Figure 6A) including Ser387 of MgcRacGAP. The anti-pS387 Ab had high affinity for PM387 and did not detect the unphosphorylated peptide M387 (Figure 6A). As shown in Figure 6B, the anti-pS387 Ab clearly immunostained the midbody of dividing cells, indicating that MgcRacGAP was phosphorylated at Ser387 as was the case in the experiments in vitro (Figures 3A and 3C) and in vivo (Figures 1A, 1B, and 2A). The anti-pS387 Ab showed no

(B) Phosphoamino acid analysis for Aurora B-induced phospho-MgcRacGAP. Phosphoamino acid analysis was done on ^{32}P-labeled MBP-MgcRacGAP protein after the incubation with Aurora B.

(C) Induction of GAP activity toward RhoA in S387D and S518D mutants of MgcRacGAP. GAP activities of MBP-fused S364D, -S387D, -S410D, -S420D, -S454D, -S486D, -S518D, and the wild-type (WT) *GAP* domain were measured toward RhoA. The results shown are the averages ±SD of three independent experiments.

(D) Phosphorylation at Ser387 and Ser410 induced by Aurora B. Aurora B-induced phosphorylation was analyzed on seven MBP-fused polypeptides coding each of ten amino acid sequences surrounding the seven Ser residues in the conserved *GAP* domain (MBP-S364, -S387, -S410, -S420, -S454, -S486, and -S518). Histone H3 protein was used as a positive control (lane 8, black arrow). MBP-S387 and MBP-S410 (lanes 2 and 3, black arrowhead) were phosphorylated by the WT-Aurora B.

(E) Reduction in GAP activities toward Rac1 in S387D and S420D mutants of MgcRacGAP. The GAP activities of MBP-fused S364D, -S387D, -S410D, -S420D, -S454D, -S486D, and -S518D were measured toward Rac1. The results shown are averages ±SD of three independent experiments.

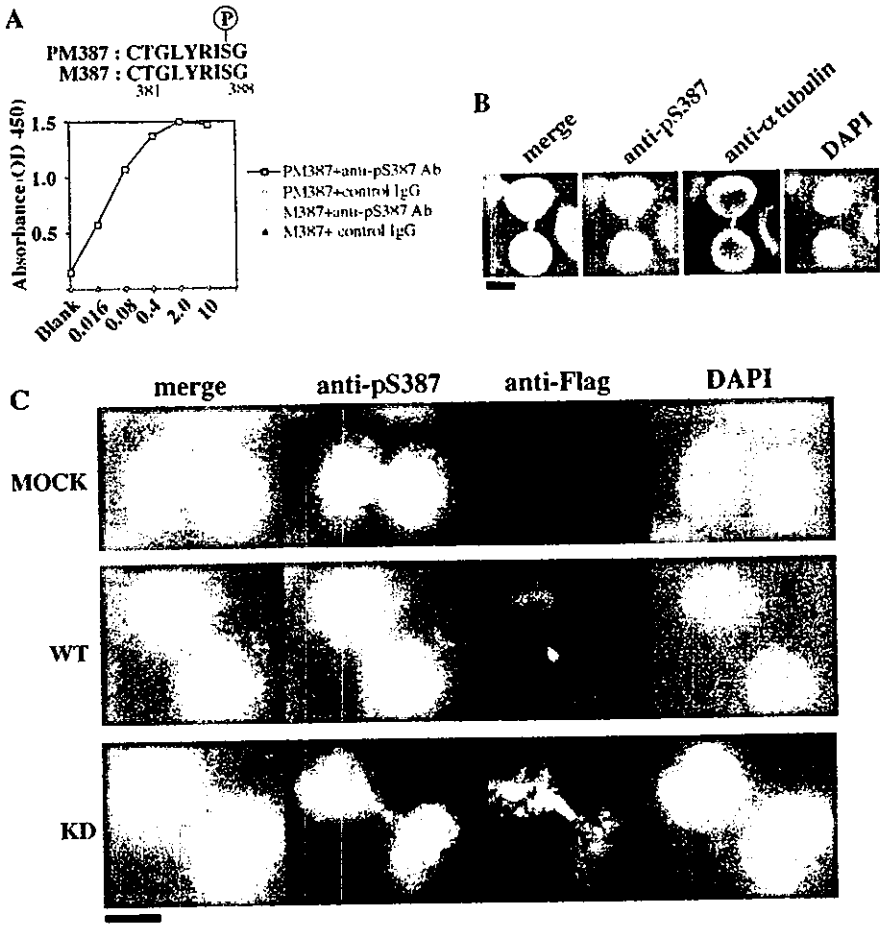

Figure 6. Localization of the Phosphorylated Form of MgcRacGAP during Cytokinesis

(A) Amino acid sequences of the synthetic peptides PM387 and M387, and specificity of the anti-phospho-Ser387 of MgcRacGAP antibody (anti-pS387 Ab) determined using ELISA. Microtiter plates were coated overnight with 60 μl (1 μg/ml) of the peptides, blocked, and reacted with the antibody. The reactivity was determined by measuring the absorbance at 450 nm.

(B) Localization of MgcRacGAP phosphorylated at Ser387 in the midbody. The anti-pS387 Ab immunoreacts with the ring-shaped structure at the midbody equator of dividing cells. HeLa cells were fixed and stained with the anti-pS387 Ab (green), anti-α-tubulin mAb (red), and DAPI (blue). The scale bar represents 10 μm.

(C) Disruption of phosphorylation of MgcRacGAP at Ser387 induced by the KD-Aurora B. HeLa cells transiently expressing the Flag-tagged WT or KD mutant of Aurora B were fixed and stained with the anti-pS387 Ab (green), anti-Flag (M2) Ab (red), and DAPI (blue). The scale bar represents 10 μm; 100× magnification.

significant immunoreactivity in the interphase cells, and no detectable signals were observed at the midbody using the anti-pS387 Ab preincubated with a 10-fold amount of PM387 (data not shown). Furthermore, overexpression of the KD-Aurora B profoundly suppressed phosphorylation of MgcRacGAP at Ser387 when compared to findings in the WT-Aurora B-transduced or MOCK-transduced cells (Figure 6C). However, the accumulation of MgcRacGAP to the midbody was not significantly affected in the KD-Aurora B-transduced cells (data not shown), suggesting that localization of MgcRacGAP to the midbody does not require Ser387 phosphorylation. These results indicate that Aurora B is indispensable for the phosphorylation of MgcRacGAP at Ser387 in vivo at the midbody. As reported (Terada et al., 1998), overexpression of the KD-Aurora B but not WT-Aurora B induces cell polyploidy in HeLa cells (data not shown).

To determine whether Ser387 phosphorylation of MgcRacGAP is critical for the completion of cytokinesis, we constructed expression vectors pME18S carrying MgcRacGAP-S387A (pME-MgcRacGAP-S387A) and MgcRacGAP-S387D (pME-MgcRacGAP-S387D), and did time-lapse studies on HeLa cells cotransfected with pME-GFP and pME-MgcRacGAP-S387A or pME-MgcRacGAP-S387D (mixed 1:5). Four of eight cells transduced with pME-MgcRacGAP-S387A failed in cytokinesis followed by cell polyploidy. A representative cell was shown in Figure 7A. The cell proceeded to the late step (2:46 and 3:00) and then the cleavage furrow regressed (3:20), resulting in polyploidy (Figure 7A). Two out of the eight cells observed underwent apoptosis,

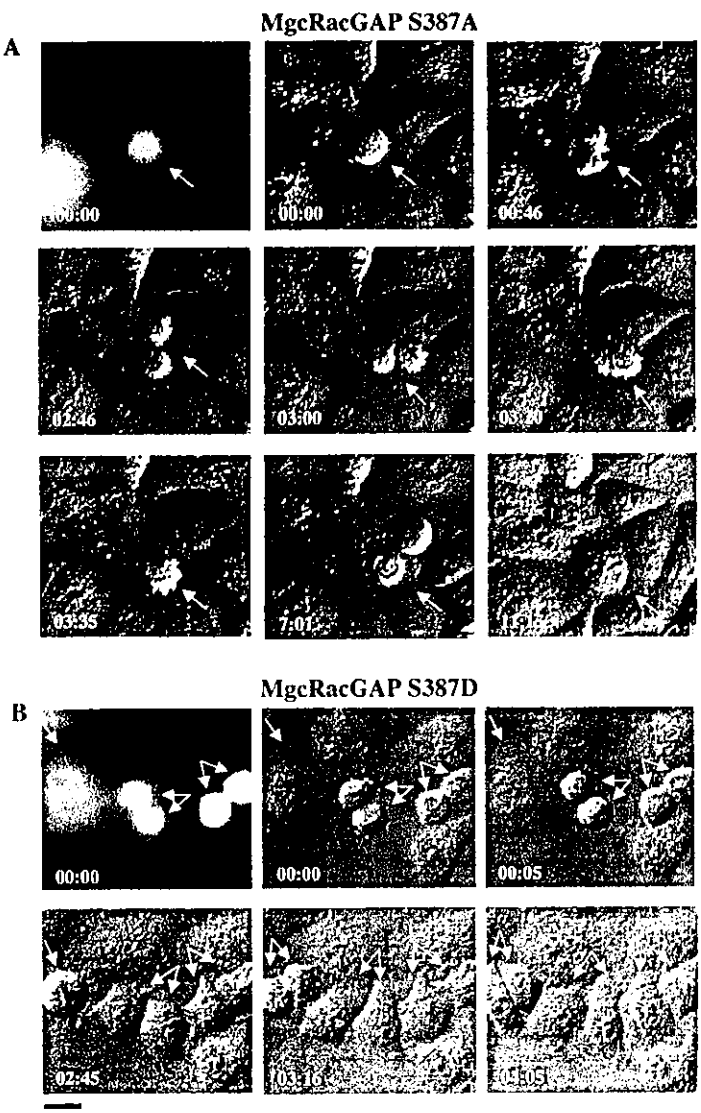

Figure 7. Phosphorylation of Ser387 on MgcRacGAP Is Indispensable for the Completion of Cytokinesis

Cell division was visualized by live cell phase contrast microscopy at a magnification of 40×. pME-MgcRacGAP-S387A (A) or pME-MgcRacGAP-S387D (B) was cotransfected with the reporter construct pME-GFP into HeLa cells. GFP-positive cells were analyzed on time-lapse studies (white arrows). The elapse time (hours and minutes) is indicated at the lower left corner of each panel. The first panels show the expression of GFP. Representative cells are shown for each stage of cell division. The scale bar represents 10 μm.

and the other two cells completed cytokinesis but with a longer time course. On the other hand, expression of MgcRacGAP-S387D did not hamper cell division (n = 8; Figure 7B; see Supplemental Movies available at http://www.developmentalcell.com/cgi/content/full/4/4/549/DC1). These results suggested that the phosphorylation of Ser387 on MgcRacGAP was essential for the completion of cytokinesis. Altogether, it is likely that cell polyploidy caused by overexpression of the KD-Aurora B is at least in part dependent on lack of phosphorylation of MgcRacGAP at Ser387.

Discussion

MgcRacGAP Works as a RhoGAP during M Phase

We (Hirose et al., 2001) and others (Jantsch-Plunger et al., 2000; Van de Putte et al., 2001) found that MgcRacGAP/CYK-4 was required for the completion of cytokinesis. We also showed that GAP activity was indispensable for cytokinesis (Hirose et al., 2001). However, it was not clear which GTPase is a target of MgcRacGAP in cytokinesis. Here we propose that Aurora B-induced phosphorylation enables MgcRacGAP to function as a RhoGAP and to play critical roles in the completion of cytokinesis as based on the following: first, Aurora B, which is one of the midbody-localized protein kinases and is also indispensable for cytokinesis, associated with and induced phosphorylation of MgcRacGAP (Figures 2A, 2B, 3A, and 6C). Second, this phosphorylation switched on a latent GAP activity of MgcRacGAP toward RhoA (Figures 4A and 4C). Because most MgcRacGAP in the midbody was phosphorylated (Figure 1A), these findings explain well why the purified *GAP* domain of MgcRacGAP did not show efficient GAP activities toward RhoA (Kawashima et al., 2000; Toure et al., 1998). Third, MgcRacGAP colocalized with RhoA on the contractile ring at the late step of cytokinesis (Figure 5, upper panels). Fourth, phosphorylation of MgcRacGAP

at Ser387 was induced by Aurora B in an in vitro system (Figure 4D) and was, at least in part, a critical switch by which MgcRacGAP acquired RhoGAP activity (Figure 4C). Moreover, this phosphorylation indeed occurred in vivo at the midbody (Figure 6B). Finally, forced expression of the KD-Aurora B induced cell polyploidy with the reduction in phosphorylation of MgcRacGAP at Ser387 (Figure 6C), and the phosphorylation at Ser387 of MgcRacGAP appeared to be indispensable for the completion of cytokinesis (Figure 7A). Therefore, it is likely that RhoA is the essential target of MgcRacGAP in cytokinesis, and inactivation of RhoA at the late step of cytokinesis is mediated by functional interactions between Aurora B and MgcRacGAP.

To our knowledge, this is the first demonstration that a GAP can exert its latent GAP activities through its phosphorylation.

MgcRacGAP Is an Essential Target of Aurora B for the Completion of Cytokinesis

In *Caenorhabditis elegans*, the Aurora B ortholog air-2 is required for the correct positioning of ZEN-4, which is a kinesin-related protein and localizes at the central spindle during mitosis (Severson et al., 2000). The cytokinesis defect in Aurora B-depleted cells was proposed to result from central spindle instability caused by the lack of ZEN-4 targeting (Kaitna et al., 2000; Severson et al., 2000). On the other hand, the situation is different in *Drosophila* and mammalian systems. In *Drosophila*, Aurora B is not required for the correct localization of Pavarotti-KLP, the *Drosophila* ZEN-4 ortholog, although RNAi inhibition of Aurora B hampers cytokinesis (Adams et al., 2001). In the mammalian system, the localization of MKLP-1/ZEN-4 as well as MgcRacGAP at the midbody was not affected by expression of the KD-Aurora B in HeLa cells (data not shown). These results suggested that cytokinesis defects seen after the inhibition of Aurora B function are not entirely due to interference with the positioning of the highly conserved KLP, and that there exist other essential targets of Aurora B in order to promote the completion of cytokinesis.

To date, several substrates and interacting proteins of Aurora B have been identified. In the mammalian system, Aurora B induces the phosphorylation of centromere protein A (CENP-A) at Ser7, and expression of both CENP-A mutants mimicking the constitutively phosphorylated (S7E) and unphosphorylated states (S7A) cause a delay at the terminal stage of cytokinesis, but do not inhibit cytokinesis (Zeitlin et al., 2001). Thus, although it is clear that the kinase activity of Aurora B is essential in cytokinesis, an essential target of Aurora B in cytokinesis has not been identified. In this report, we provide evidence that MgcRacGAP is a candidate for one of the Aurora B targets essential for the completion of cytokinesis.

Cytokinesis is disrupted by the expression of a dominant active mutant of RhoA and a kinase-defective (KD) mutant of Aurora B as well as a GAP-inactive mutant of MgcRacGAP, inducing multinucleated cells (Drechsel et al., 1997; Hirose et al., 2001; Terada et al., 1998). Our present findings indicating a signaling pathway connecting Aurora B, MgcRacGAP, and RhoA can explain how a KD mutant of Aurora B or a GAP-inactive mutant of MgcRacGAP induces cell polyploidy; cell polyploidy induced by a function-defective mutant of Aurora B or MgcRacGAP may depend on lack of machinery to inactivate RhoA. Forced expression of the KD-Aurora B led to frequent cell polyploidization with reduction in phosphorylation of MgcRacGAP at Ser387 (Figure 6C). Overexpression of MgcRacGAP-S387A but not MgcRacGAP-S387D led to frequent cell polyploidy (Figures 7A and 7B). Accordingly, the disruption of normal cell division induced by the KD-Aurora B would, at least in part, depend on the reduction of phosphorylation of the Ser387 residue in MgcRacGAP. S387A mutant still had GAP activities toward Rac1/Cdc42 but no GAP activity toward RhoA, and S387D mutant lost GAP activities toward Rac1/Cdc42 but had a detectable GAP activity toward RhoA (Figures 4C and 4E, and data not shown). We previously demonstrated that overexpression of the GAP-inactive mutant MgcRacGAP-R385A, which had no GAP activity toward Rac1/Cdc42 or RhoA, induced frequent cell polyploidy (Hirose et al., 2001). It was notable that, whereas both MgcRacGAP-S387D and MgcRacGAP-R385A lost GAP activities toward Rac1 and Cdc42, only MgcRacGAP-S387D with a detectable RhoGAP activity induced completion of cytokinesis. These results strongly indicate that the GAP activity of MgcRacGAP-S387D, albeit low, is critical for the completion of cytokinesis.

We conclude that MgcRacGAP plays essential roles in cytokinesis as a RhoGAP at the late step of cytokinesis, based on observations that MgcRacGAP clearly colocalized with RhoA on the contractile ring, and that the Aurora B-dependent phosphorylation of MgcRacGAP at Ser387 resulted in stimulation of its latent GAP activity toward RhoA and was indispensable for the completion of cytokinesis.

Experimental Procedures

Cell Culture and Midbody Isolation

HeLa cells were grown in DMEM supplemented with 5% fetal calf serum (FCS). Cells were seeded at 2×10^5 cells per 10 cm dish and were collected after EDTA treatment on day 3 during the log phase. Midbodies were isolated from the collected cells as described (Bellissent-Waydelich et al., 1999; Mullins and McIntosh, 1982). The isolated midbodies were used for immunoblotting experiments, and in some experiments we treated them with VHR (0.5 μg/ml; Ishibashi et al., 1992) for 2 hr at 30°C in the absence or presence of the protein phosphatase inhibitor sodium vanadate (Na_3VO_4), followed by immunoblotting.

Metabolic Labeling, Immunoprecipitation, and Western Blot Analysis

For metabolic labeling, cells were washed with phosphatase-free RPMI medium (GIBCO-BRL) and incubated with ^{32}P-labeled orthophosphoric acid for 6 hr, as described (Deng et al., 2000). After the cells were washed with ice-cold Tris-buffered saline (TBS), the midbodies were collected and lysed in a detergent buffer. MgcRacGAP was immunoprecipitated as described previously (Kawashima et al., 2001). The samples were subjected to SDS-PAGE, transferred to a nitrocellulose membrane, and exposed to Kodak X-Omat film for 24 hr at −80°C. In order to detect the amount of MgcRacGAP protein, the filters were then probed with an anti-MgcRacGAP antibody (Ab) (Hirose et al., 2001) and developed using an ECL kit (Amersham).

Synchronization of the Cell Cycle

HeLa cells were seeded into a 6 cm dish at 1×10^5 cells/dish. Synchronization of the cell cycle was achieved by double-thymidine

block (Lee et al., 1995). HeLa cells in the exponential growth phase were exposed to 2.5 mM thymidine in DMEM/5% FCS for 15 hr and then incubated in fresh medium for 9 hr. Cells were once again exposed to 2.5 mM thymidine for 15 hr and were cultured in fresh DMEM containing 10% FCS. After 6 hr, nocodazole was added at the final concentration of 80 ng/ml, and the culture was continued for another 6 hr. Round mitotic cells were purified by the shake-off procedure, as described. Collected cells were suspended in fresh DMEM containing 10% FCS to release from the nocodazole arrest. At 0, 45, 90, and 180 min after the release, the cells were harvested and subjected to analyses.

Glutathione S-Transferase Pull-Down Assays

Using purified glutathione S-transferase (GST)-fused wild-type (WT) Aurora B, GST-fused kinase-defective (KD) mutant of Aurora B, or GST alone against purified maltose binding protein (MBP)-fused MgcRacGAP, GST pull-down assays were performed in buffer A (25 mM Tris [pH 7.5], 2 mM $MgCl_2$, 200 μM ATP, 0.1 μM calyculin A, 1% Nonidet P-40). GST beads were washed three times with buffer A. Proteins bound to beads were analyzed using SDS-PAGE followed by immunoblotting with the anti-MgcRacGAP Ab.

Immunostaining and Antibodies

HeLa cells were immunostained as described (Hirose et al., 2001). The antibodies, mouse anti-AIM-1 (Transduction Laboratories), affinity-purified rabbit anti-MgcRacGAP, mouse anti-RhoA (Santa Cruz), mouse anti-Cdc42 (Transduction Laboratories), mouse anti-Rac1 (Transduction Laboratories), mouse anti-α-tubulin (Sigma), mouse anti-Flag (M2) (Sigma), and rabbit anti-phospho-Ser387 of MgcRacGAP (anti-pS387), were used as the first antibody. FITC-conjugated goat anti-rabbit Ig (Wako) and rhodamine-conjugated goat anti-mouse Ig (Sigma) were used as the second antibody. The coverslips were washed six times with PBS. After the final wash, the coverslips were mounted with glycerin containing para-phenylenediamine (PPD) at 10 mg/ml and DAPI (4′6-diamino-2-phenylindole) at 1 μg/ml. The labeled cells were examined using a FLUOVIEW FV300 confocal microscope (Olympus) or a fluorescence microscope IX70 (Olympus) equipped with a SenSys/OL cold CCD camera (Olympus) and IP-Lab software (Signal Analytics).

In Vitro Phosphorylation of MgcRacGAP

The phosphorylation reaction of MgcRacGAP by glutathione S-transferase (GST)-fused Aurora B/AIM-1 kinase was observed for 30 min at 25°C in 100 μl of the reaction mixture (25 mM Tris [pH 7.5], 2 mM $MgCl_2$, 100 μM ATP, 100 μM [γ-^{32}P]ATP, 0.1 μM calyculin A, 80 μg/ml purified WT-Aurora B or KD mutant [Terada et al., 1998], 300 μg/ml purified MgcRacGAP or GAP domain of MgcRacGAP fused to maltose binding-protein [MBP]). After the reaction, the mixtures were boiled in Laemmli's sample buffer (Laemmli, 1970) and subjected to SDS-PAGE. In some experiments, to obtain an isotope-free phosphorylated form of purified GAP domain, the reaction was extended for 2 hr at 25°C in 100 μl of 25 mM Tris (pH 7.5), 2 mM $MgCl_2$, 100 μM ATP, 0.1 μM calyculin A, 80 μg/ml purified WT- or KD-Aurora B, 300 μg/ml purified GAP domain. The reaction mixtures were subjected to GTP hydrolysis assay.

GTP Hydrolysis Assays

GTP hydrolysis assays were performed as described (Kawashima et al., 2000). Typically, 100% of [γ-^{32}P]GTP bound to GTPases is around 25,000 cpm. During the step of GTP hydrolysis, the GTP hydrolysis assay was done in the presence of the reaction mixture containing the GAP domain (1.5 μg) preincubated with the WT- or KD-Aurora B. The GTP exchange reaction during the GTP hydrolysis step was examined using [α-^{32}P]GTP-preloaded GTPases under similar conditions, and was not significantly affected by the presence of MgcRacGAP (data not shown).

Phosphoamino Acid Analysis

MgcRacGAP proteins phospholabeled by Aurora B using [γ-^{32}P] ATP were resolved in a 10% SDS-polyacrylamide gel. ^{32}P-labeled MgcRacGAP proteins were excised from the SDS-polyacrylamide gel and subjected to phosphoamino acid analysis as described (Boyle et al., 1991). The ^{32}P-labeled MgcRacGAP was two-dimensionally electrophoresed for 20 min at 1.5 kV in a pH 1.9 buffer (first dimension) and for 16 min at 1.3 kV in a pH 3.5 buffer (second dimension) using the HTLE7000 apparatus (CBS Scientific). The plate was air dried and then exposed to presensitized Kodak XAR film with an intensifying screen at −70°C for 14 days.

Production of Site- and Phosphorylation State-Specific Antibody against MgcRacGAP

The phosphopeptide Cys-Thr-Gly-Leu-Tyr-Arg-Ile-phospho-Ser^{387}-Gly (PM387) and unphosphorylated peptide Cys-Thr-Gly-Leu-Tyr-Arg-Ile-Ser^{387}-Gly (M387) were chemically synthesized as an antigen by the Peptide Institute. Antibodies against PM387 were prepared by injecting two rabbits with PM387 coupled to keyhole limpet hemocyanin, mixed with RIBI adjuvant system R-730 (RIBI Immunochem Research). Monospecific antibodies against PM387 were purified from the obtained serum by two-step chromatography: absorption in M387-coupled sepharose (MBL) and then affinity chromatography on PM387-coupled sepharose. Purified anti-PM387 antibodies from two rabbits gave similar immunoreactivity; thus one of these antibodies with a higher titer was referred to as anti-pS387 Ab (0.66 mg/ml) and was used for the following experiments.

DNA Transfection

HeLa cells were grown and seeded in a 6 cm dish at 1×10^6/dish. On the following day, the cells were transiently transfected with plasmids encoding the Flag-tagged WT or KD mutant form of Aurora B using LipofectAMINE-PLUS (GIBCO-BRL) according to manufacturer's recommendations.

Acknowledgments

We thank Dr. Y. Kaziro for critical reading of the manuscript, Dr. S. Imajoh-Ohmi for valuable discussions, and M. Ohara for language assistance. The Division of Hematopoietic factors is supported by the Chugai Pharmaceutical Company. This work was also supported by grants from the Ministry of Education, Culture, Sports, Science, and Technology of Japan and by the Ministry of Health, Labor, and Welfare of Japan, and by a grant from the NAKAJIMA foundation.

Received: October 15, 2002
Revised: February 7, 2003
Published: April 7, 2003

References

Adams, R.R., Maiato, H., Earnshaw, W.C., and Carmena, M. (2001). Essential roles of *Drosophila* inner centromere protein (INCENP) and aurora B in histone H3 phosphorylation, metaphase chromosome alignment, kinetochore disjunction, and chromosome segregation. J. Cell Biol. *153*, 865–880.

Bellissent-Waydelich, A., Vanier, M.T., Albiges-Rizo, C., and Simon-Assmann, P. (1999). Talin concentrates to the midbody region during mammalian cell cytokinesis. J. Histochem. Cytochem. *47*, 1357–1368.

Boyle, W.J., van der Geer, P., and Hunter, T. (1991). Phosphopeptide mapping and phosphoamino acid analysis by two-dimensional separation on thin-layer cellulose plates. Methods Enzymol. *201*, 110–149.

Deng, X., Ruvolo, P., Carr, B., and May, W.S., Jr. (2000). Survival function of ERK1/2 as IL-3-activated, staurosporine-resistant Bcl2 kinases. Proc. Natl. Acad. Sci. USA *97*, 1578–1583.

Drechsel, D.N., Hyman, A.A., Hall, A., and Glotzer, M. (1997). A requirement for Rho and Cdc42 during cytokinesis in *Xenopus* embryos. Curr. Biol. *7*, 12–23.

Hall, A. (1998). Rho GTPases and the actin cytoskeleton. Science *279*, 509–514.

Hirose, K., Kawashima, T., Iwamoto, I., Nosaka, T., and Kitamura, T. (2001). MgcRacGAP is involved in cytokinesis through associating with mitotic spindle and midbody. J. Biol. Chem. *276*, 5821–5828.

Hsu, J.Y., Sun, Z.W., Li, X., Reuben, M., Tatchell, K., Bishop, D.K., Grushcow, J.M., Brame, C.J., Caldwell, J.A., Hunt, D.F., et al. (2000).

Mitotic phosphorylation of histone H3 is governed by Ipl1/aurora kinase and Glc7/PP1 phosphatase in budding yeast and nematodes. Cell *102*, 279–291.

Ishibashi, T., Bottaro, D.P., Chan, A., Miki, T., and Aaronson, S.A. (1992). Expression cloning of a human dual-specificity phosphatase. Proc. Natl. Acad. Sci. USA *89*, 12170–12174.

Jantsch-Plunger, V., Gonczy, P., Romano, A., Schnabel, H., Hamill, D., Schnabel, R., Hyman, A.A., and Glotzer, M. (2000). CYK-4: a Rho family gtpase activating protein (GAP) required for central spindle formation and cytokinesis. J. Cell Biol. *149*, 1391–1404.

Kaitna, S., Mendoza, M., Jantsch-Plunger, V., and Glotzer, M. (2000). Incenp and an aurora-like kinase form a complex essential for chromosome segregation and efficient completion of cytokinesis. Curr. Biol. *10*, 1172–1181.

Kawashima, T., Hirose, K., Satoh, T., Kaneko, A., Ikeda, Y., Kaziro, Y., Nosaka, T., and Kitamura, T. (2000). MgcRacGAP is involved in the control of growth and differentiation of hematopoietic cells. Blood *96*, 2116–2124.

Kawashima, T., Murata, K., Akira, S., Tonozuka, Y., Minoshima, Y., Feng, S., Kumagai, H., Tsuruga, H., Ikeda, Y., Asano, S., et al. (2001). STAT5 induces macrophage differentiation of M1 leukemia cells through activation of IL-6 production mediated by NF-κB p65. J. Immunol. *167*, 3652–3660.

Kimura, K., Tsuji, T., Takada, Y., Miki, T., and Narumiya, S. (2000). Accumulation of GTP-bound RhoA during cytokinesis and a critical role of ECT2 in this accumulation. J. Biol. Chem. *275*, 17233–17236.

Kishi, K., Sasaki, T., Kuroda, S., Itoh, T., and Takai, Y. (1993). Regulation of cytoplasmic division of *Xenopus* embryo by rho p21 and its inhibitory GDP/GTP exchange protein (rho GDI). J. Cell Biol. *120*, 1187–1195.

Kiyono, M., Kaziro, Y., and Satoh, T. (2000). Induction of rac-guanine nucleotide exchange activity of Ras-GRF1/CDC25(Mm) following phosphorylation by the nonreceptor tyrosine kinase Src. J. Biol. Chem. *275*, 5441–5446.

Laemmli, U.K. (1970). Cleavage of structural proteins during the assembly of the head of bacteriophage T4. Nature *227*, 680–685.

Lee, K.S., Yuan, Y.L., Kuriyama, R., and Erikson, R.L. (1995). Plk is an M-phase-specific protein kinase and interacts with a kinesin-like protein, CHO1/MKLP-1. Mol. Cell. Biol. *15*, 7143–7151.

Mabuchi, I., Hamaguchi, Y., Fujimoto, H., Morii, N., Mishima, M., and Narumiya, S. (1993). A rho-like protein is involved in the organisation of the contractile ring in dividing sand dollar eggs. Zygote *1*, 325–331.

Mullins, J.M., and McIntosh, J.R. (1982). Isolation and initial characterization of the mammalian midbody. J. Cell Biol. *94*, 654–661.

Raymond, K., Bergeret, E., Dagher, M.C., Breton, R., Griffin-Shea, R., and Fauvarque, M.O. (2001). The Rac GTPase-activating protein RotundRacGAP interferes with Drac1 and Dcdc42 signalling in *Drosophila melanogaster*. J. Biol. Chem. *276*, 35909–35916.

Severson, A.F., Hamill, D.R., Carter, J.C., Schumacher, J., and Bowerman, B. (2000). The aurora-related kinase AIR-2 recruits ZEN-4/CeMKLP1 to the mitotic spindle at metaphase and is required for cytokinesis. Curr. Biol. *10*, 1162–1171.

Takaishi, K., Sasaki, T., Kato, M., Yamochi, W., Kuroda, S., Nakamura, T., Takeichi, M., and Takai, Y. (1994). Involvement of Rho p21 small GTP-binding protein and its regulator in the HGF-induced cell motility. Oncogene *9*, 273–279.

Tatsumoto, T., Xie, X., Blumenthal, R., Okamoto, I., and Miki, T. (1999). Human ECT2 is an exchange factor for Rho GTPases, phosphorylated in G2/M phases, and involved in cytokinesis. J. Cell Biol. *147*, 921–928.

Terada, Y., Tatsuka, M., Suzuki, F., Yasuda, Y., Fujita, S., and Otsu, M. (1998). AIM-1: a mammalian midbody-associated protein required for cytokinesis. EMBO J. *17*, 667–676.

Toure, A., Dorseuil, O., Morin, L., Timmons, P., Jegou, B., Reibel, L., and Gacon, G. (1998). MgcRacGAP, a new human GTPase-activating protein for Rac and Cdc42 similar to *Drosophila* rotundRacGAP gene product, is expressed in male germ cells. J. Biol. Chem. *273*, 6019–6023.

Van de Putte, T., Zwijsen, A., Lonnoy, O., Rybin, V., Cozijnsen, M., Francis, A., Baekelandt, V., Kozak, C.A., Zerial, M., and Huylebroeck, D. (2001). Mice with a homozygous gene trap vector insertion in mgcRacGAP die during pre-implantation development. Mech. Dev. *102*, 33–44.

Zeitlin, S.G., Shelby, R.D., and Sullivan, K.F. (2001). CENP-A is phosphorylated by Aurora B kinase and plays an unexpected role in completion of cytokinesis. J. Cell Biol. *155*, 1147–1157.

Article

Control of axon elongation via an SDF-1α/Rho/mDia pathway in cultured cerebellar granule neurons

Yoshiki Arakawa,[1,2] Haruhiko Bito,[1,3,4] Tomoyuki Furuyashiki,[1] Takahiro Tsuji,[1] Sayaka Takemoto-Kimura,[1] Kazuhiro Kimura,[1] Kazuhiko Nozaki,[2] Nobuo Hashimoto,[2] and Shuh Narumiya[1]

[1]Department of Pharmacology and [2]Department of Neurosurgery, Kyoto University Faculty of Medicine, and [3]PRESTO-Japan Science and Technology Corporation, Sakyo-ku, Kyoto 606-8315, Japan
[4]Department of Neurochemistry, University of Tokyo Graduate School of Medicine, Bunkyo-ku, Tokyo 113-0033, Japan

Rho–GTPase has been implicated in axon outgrowth. However, not all of the critical steps controlled by Rho have been well characterized. Using cultured cerebellar granule neurons, we show here that stromal cell–derived factor (SDF)-1α, a neural chemokine, is a physiological ligand that can turn on two distinct Rho-dependent pathways with opposite consequences. A low concentration of the ligand stimulated a Rho-dependent pathway that mediated facilitation of axon elongation. In contrast, Rho/ROCK activation achieved by a higher concentration of SDF-1α caused repression of axon formation and induced no more increase in axon length. However, even at this higher concentration a Rho-dependent axon elongating activity could be recovered upon removal of ROCK activity using Y-27632. SDF-1α–induced axon elongating activity under ROCK inhibition was replicated by the dominant-active form of the mammalian homologue of the *Drosophila* gene Diaphanous (mDia)1 and counteracted by its dominant-negative form. Furthermore, RNAi knockdown of mDia1 abolished SDF-1α–induced axon elongation. Together, our results support a critical role for an SDF-1α/Rho/mDia1 pathway in mediating axon elongation.

Introduction

It has been widely accepted that rearrangement of actin and microtubule cytoskeleton lies at the heart of neuronal morphogenesis (Tanaka and Sabry, 1995). Drastic changes in neuronal shape occur immediately after the exit of neuronal cells from mitotic cycles, during embryonic and postnatal development. Process formation/extension and cell body migration must be spatially and temporally orchestrated in order to achieve patterned formation of neuronal cell layers and appropriate generation of synaptic circuits (Goodman and Shatz, 1993; Tessier-Lavigne and Goodman, 1996; Van Vactor and Flanagan, 1999).

A dynamic morphological alteration is initiated during the acquisition of neuronal polarity and must continue until the completion of synaptogenesis. Recent findings indicate a critical role for the antagonism between Rac– and Rho–GTPases in these events (Narumiya et al., 1997; Hall, 1998; Luo, 2000; Dickson, 2001). A large body of work has now established that several soluble or transmembranous guidance molecule systems can exhibit either chemorepulsion or chemoattraction toward axonal growth cones, at least in part, via coupling to either Rho or Rac, respectively. Such systems include EphrinA (Shamah et al., 2001), EphB reverse signaling (Lu et al., 2001), Sema4D/PlexinB (Driessens et al., 2001; Swiercz et al., 2002), Sema3A/PlexinA-Neuropilin (Jin and Strittmatter, 1997; Liu and Strittmatter, 2001; Jurney et al., 2002), Netrin/DCC (Li et al., 2002), Slit/Robo (Wong et al., 2001), and neurotrophins/p75/trk (Yamashita et al., 1999; Huang and Reichardt, 2001; Ozdinler and Erzurumlu, 2001; Nusser et al., 2002). Thus, antagonistic interactions and hierarchical cascades between distinct small GTPases had been considered as most likely ways by which distinct gradient cues could be decoded into reliable maps of afferents projecting into one specific area of the central nervous system (CNS).*

However, to date, a clear understanding regarding what specific effectors of the small GTPases contribute to each of these opposing signaling events is still missing. Furthermore, whether Rho always antagonized with Rac remains controversial (Sebok et al., 1999; Bashaw et al., 2001).

The online version of this article includes supplemental material.

Address correspondence to Shuh Narumiya, Dept. of Pharmacology, Kyoto University Faculty of Medicine, Yoshida, Sakyo-ku, Kyoto 606-8315, Japan. Tel.: 81-75-753-4392. Fax: 81-75-753-4693. E-mail: snaru@mfour.med.kyoto-u.ac.jp

Key words: mDia; Rho; axon elongation; cerebellar granule neuron; SDF-1α

*Abbreviations used in this paper: CRIB, Cdc42/Rac interactive binding; CNS, central nervous system; DA, dominant-active; DN, dominant-negative; EGFP, enhanced GFP; EGL, external granule cell layer; IGL, internal granule cell layer; mDia, mammalian homologue of the *Drosophila* gene Diaphanous; P, postnatal day; PAK, p21-associated kinase; RBD, Rho-binding domain; RNAi, RNA interference; siRNA, short interfering double stranded RNA oligomer; SDF, stromal cell–derived factor.

The Journal of Cell Biology, Volume 161, Number 2, April 28, 2003 381–391
http://www.jcb.org/cgi/doi/10.1083/jcb.200210149

Supplemental Material can be found at:
http://www.jcb.org/cgi/content/full/jcb.200210149/DC1

The rodent cerebellar granule cells represent a highly advantageous resource to study in detail the molecular sequence of events controlling axonogenesis, neuronal migration, dendritogenesis, and synaptogenesis. Indeed, each of these steps that is critical for neuronal maturation and circuit formation occurs in an organized and sequential fashion in the cerebellum during the postnatal 3 wk after birth (Altman and Bayer, 1996; Hatten, 1999). Many of these steps involve dramatic changes in neuronal morphology, yet previous studies indicated that many of their features could be recapitulated, at least in part, in primary culture (Powell et al., 1997; Bito et al., 2000; Yamasaki et al., 2001; Yacubova and Komuro, 2002).

Previous investigation of molecular determinants involved in axon formation in cerebellar granule cells, from our laboratory and others, have begun to uncover the critical importance of pia–granule cell interaction (Bhatt et al., 2000) on one hand and control of actin dynamics on the other (Bito et al., 2000; Yamasaki et al., 2001). Thus, we considered the possibility that a factor supplied by the pia mater may be involved in the signaling pathway controlling axon initiation and elongation. One candidate factor we tested was stromal cell–derived factor (SDF)-1α, a chemokine heavily expressed in the pia mater and chemoattractant for migration of cerebellar granule cells (Lu et al., 2001; Klein et al., 2001; Tham et al., 2001; Zhu et al., 2002). Our interest was prompted by the striking phenotype of the knockout mice lacking either SDF-1α (Ma et al., 1998) or its cognate receptor CXCR4 (Ma et al., 1998; Zou et al., 1998). In both lines of mice, the formation of the cerebellar granule cell layers was abolished. This suggested that early events in cerebellar granule cell morphogenesis, such as axon initiation, axon elongation, or migration of the cell body, might be severely perturbed in the absence of SDF-1α signaling.

However, whether SDF-1α could stimulate axon formation via direct control of actin cytoskeletal signaling mechanisms in cerebellar granule cells has not been demonstrated. Here we show that SDF-1α activates Rho but not Rac small GTPase in cerebellar granule cells. A low concentration (100 ng/ml) of SDF-1α induced significant amount of axon outgrowth in a C3 exoenzyme–sensitive fashion. In contrast, at a higher concentration SDF-1α rather repressed axon formation in a Rho-dependent manner. However, Y-27632 treatment was sufficient to uncover an axon elongating activity even under high dose of SDF-1α. Thus, SDF-1α stimulated two distinct opposing Rho effectors: a novel Rho effector, which promoted axon elongation, and ROCK to inhibit axonogenesis. The facilitatory effect of SDF-1α in the presence of Y-27632 could be mimicked by overexpressing a dominant-active (DA) form of the mammalian homologue of the *Drosophila* gene Diaphanous (mDia)1, a Rho effector involved in control of actin polymerization during cell polarization and directed cell growth. This dominant activation of mDia was dependent on intact Rac activity. Furthermore, the axon outgrowth induced by SDF-1α could be antagonized either by overexpression of a dominant interfering mutant or by RNAi knockdown of mDia1. Thus, we identify a novel function for mDia1 as a critical Rho effector–mediating SDF-1α–dependent axon elongation in concert with Rac.

Results

A pial chemokine SDF-1α triggers axon elongation via Rho early in culture in cerebellar granule cells

We tested whether SDF-1α was able to trigger any axon growth and whether this morphological change correlated, at least in part, with an alteration in either Rho or Rac activity in cultured cerebellar granule cells, where axonogenesis is well known to precede dendritogenesis. A 12-h exposure to SDF-1α at a concentration of 100 ng/ml induced a significant increase in the mean length of first appearing process compared with control (Fig. 1, A and B; Video 1, avail-

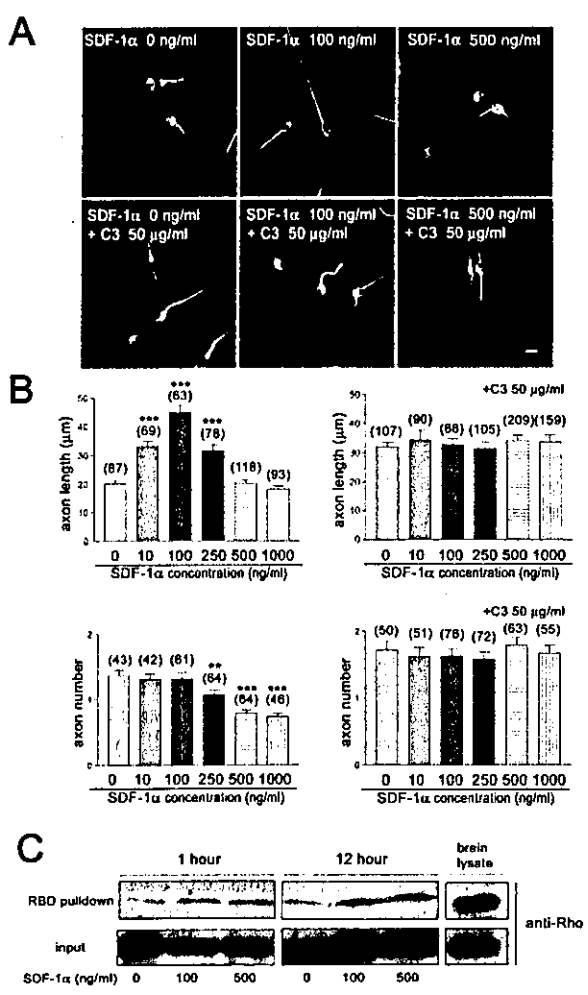

Figure 1. **SDF-1α facilitates axon elongation via a Rho-dependent pathway.** (A) Facilitation of axon elongation by 12-h exposure to SDF-1α (top). SDF-1α–induced facilitation is blocked by C3 treatment (bottom), indicating the existence of a Rho-dependent mode of neurite extension. β-tubulin immunostaining was employed to completely trace the entire length of axons. (B) Axon elongating activity induced by SDF-1α reveals a bell-shaped response curve, whereas axon numbers are reduced at only higher concentrations. SDF-1α effect on axon length and number are both blocked by C3 treatment. $n \approx 42$–209. (C) 1- or 12-h exposure to SDF-1α (100 or 500 ng/ml) leads to a substantial increase in the amount of GTP-bound Rho (RBD pulldown) but not that of GTP-bound Rac (unpublished data) in cerebellar granule cells. **P < 0.01; ***P < 0.001. Bar, 5 μm.

able at http://www.jcb.org/cgi/content/full/jcb.200210149/DC1), while having no effect on axon number (Fig. 1, A and B). This effect was abolished in the presence of C3 exoenzyme, a Rho inhibitor (Fig. 1, A and B). SDF-1α promoted a bell-shaped response in axon elongation with a peak effect at 100 ng/ml (Fig. 1, A and B). However, at a larger concentration this axon outgrowth effect was abolished and indistinguishable from the control (Fig. 1 B). In contrast, SDF-1α treatment significantly reduced axon number at concentrations over 250 ng/ml. Presence of C3 exoenzyme completely flattened either response (Fig. 1 B). Together, this indicated that SDF-1α may promote axon elongation via Rho, at least at lower concentrations, whereas it inhibited initiation of axon at higher concentrations. The reduction in SDF-1α–dependent axon growth with the maximal concentration of SDF-1α was unlikely to be caused by receptor desensitization or inactivation, since we confirmed that axon numbers were now negatively affected at the same dose. Furthermore, either 1- or 12-h exposure to either 100 or 500 ng/ml SDF-1α was accompanied with a similarly strong elevation in the amount of GTP-bound form of Rho (Fig. 1 C), whereas no apparent increase was discerned for GTP-bound Rac (unpublished data) as determined by pull-down assays using either a GST-fused Rho-binding domain (RBD) of Rhotekin or a GST-fused Cdc42/Rac interactive binding (CRIB) domain of p21-associated kinase (PAK) were performed (Ren et al., 1999; Tsuji et al., 2002). These results indicate the possibility that stimulation of Rho pathway with a physiological ligand such as SDF-1α may mediate axon elongation.

Antagonism between a Rho-activated axon elongating pathway and ROCK-mediated control of axonogenesis

To test whether the biphasic responsiveness could be accounted for by the existence of distinct thresholds of activation of two separate Rho effectors, we carefully reexamined the dose–response relationship between C3 concentration and resulting axon length. The sampling number was increased substantially in order to detect even small differences that might have been overlooked before. At 10 μg/ml of C3, a significant increase in axon length and number was achieved (Fig. 2). When the dose was augmented to 30–50 μg/ml, this facilitation in axon length was substantially diminished compared with 10 μg/ml treatment, though a small but significant net increase was still detectable; however, no additional effect was seen on axon number (Fig. 2). Therefore, different concentrations of active Rho were likely to gear two distinct pathways, repression and facilitation of axon extension, via two distinct Rho effectors. In contrast, only one Rho effector was likely to contribute to axon number control (Fig. 2), consistent with our previous work (Bito et al., 2000). A similar C3 dose–response curve was also reported in PC-12 cells (Winton et al., 2002).

What are these two Rho effectors? The finding that SDF-1α seemed to antagonize axonogenesis at higher doses in a Rho-dependent manner (Fig. 1 B) was in keeping with our previous finding that Rho/ROCK signaling critically regulates axon numbers (Bito et al., 2000). To test whether ROCK, a Rho-associated kinase (Narumiya et al., 1997; Bito et al., 2000; Ishizaki et al., 2000), was indeed mediating the SDF-1α effect, we bath-applied 50 μM Y-27632, a potent

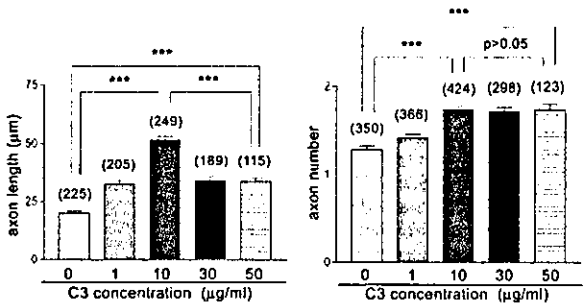

Figure 2. **Distinct C3 dose effectiveness on axon elongation and axon number in cultured cerebellar granule neurons.** Axon elongation reveals a bell-shaped C3 responsiveness consistent with the presence of two opposing effects downstream of Rho. However, the C3 effect on axon number is saturated at doses over 10 μg/ml. $n \approx 115$–424; ***$P < 0.001$.

and selective ROCK inhibitor (Uehata et al., 1997; Ishizaki et al., 2000). As expected, treatment with Y-27632 reversed the negative SDF-1α effect on axon numbers, indicating that SDF-1α is indeed able to activate ROCK (Fig. 3, A and B). Surprisingly, however, exposure to SDF-1α in the presence of the ROCK inhibitor now resulted in a significant net increase in axon extension (Fig. 3, A and B). Thus, SDF-1α activated a novel ROCK-independent, yet C3-sensitive, effector pathway that was coupled to axon elongation.

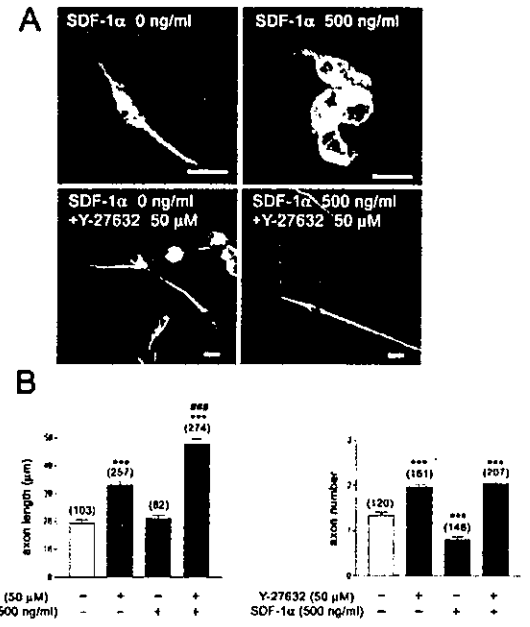

Figure 3. **SDF-1α–induced axon elongation is antagonized by ROCK.** 12-h exposure to high concentration (500 ng/ml) of SDF-1α represses axonogenesis (A, top, and B, right). Addition of 50 μM Y-27632, a specific ROCK inhibitor, blocked this SDF-1α–induced inhibition of axonogenesis (A, bottom, and B, right). Under the same condition, SDF-1α significantly facilitated axon elongation in ROCK-inhibited neurons (B, left), while having little effect on axon numbers (B, right). $n \approx 82$–74. ***Compared with untreated cells or ###compared with Y-27632-treated cells; $P < 0.001$. Bars, 5 μm.

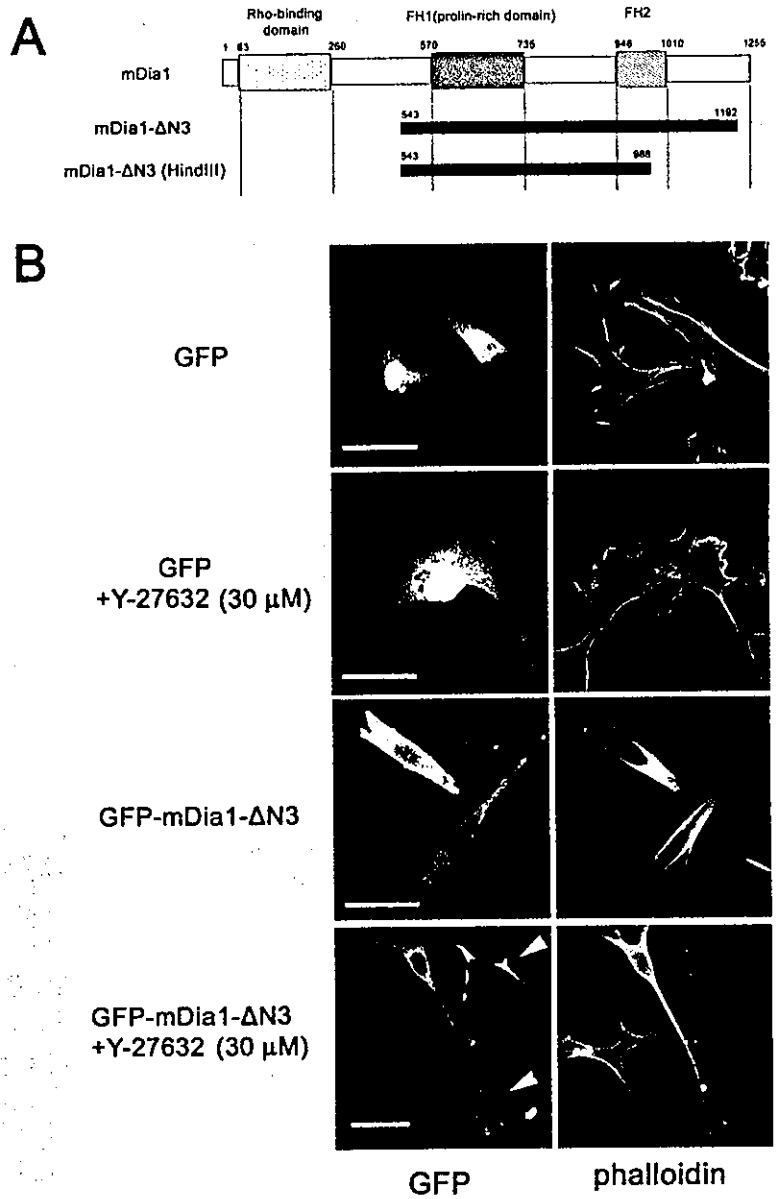

Figure 4. **A putative role for mDia1 in facilitated process outgrowth.** (A) Domain structure of wild-type and dominant mutant constructs of mDia1. (B) Coupling of elevated mDia1 activity (by overexpression of mDia1-ΔN3) with lower ROCK activity (in the presence of Y-27632) is sufficient to induce elongated axon-like processes in Swiss3T3 cells. Note the high amount of F-actin stained with phalloidin in the thin processes (arrowheads) of the GFP-mDia1-ΔN3–expressing cells. Bars, 50 μm.

The Rho effector mDia1, a regulator of actin polymerization, is heavily expressed in the external granule cell layer during early postnatal development and positively regulates axon outgrowth

Recently, mDia was found to be a critical Rho effector that may predominantly act as an inducer/regulator of actin polymerization in HeLa cells and may be required for establishment of cell polarity and directed growth (Watanabe et al., 1997; Ishizaki et al., 2001; Ozaki-Kuroda et al., 2001; Tsuji et al., 2002). Indeed, we found that Swiss3T3 cells can elongate prolonged neurite-like processes best when higher mDia activity was achieved by overexpression a DA form of mDia1 (mDia1-ΔN3; Fig. 4 A; Ishizaki et al., 2001) and was coupled with lower ROCK activity in the presence of 30 μM Y-27632 (Fig. 4 B), consistent with previous work from our laboratory (Tsuji et al., 2002).

We also found that expression of mDia1 coincided with early axonogenesis in postnatal cerebellum in mice (Fig. 5, A and B). Immunohistochemical analysis showed that mDia1 was especially abundant in postnatal day 1 (P1) cerebellum at and beneath the external granule cell layer where the earliest events in axonogenesis occurred (Fig. 5 B). In round cerebellar granule cells, mDia1 protein was already colocalized with F-actin and tubulin at spots where an axon was likely to initiate (Fig. 5 C). After axon outgrowth started, mDia1 was heavily enriched at the base of early initiating process and within its growth cones (Fig. 5 C, arrowheads) in close spatial vicinity with actin filaments and microtubules (Figs. 5 C).

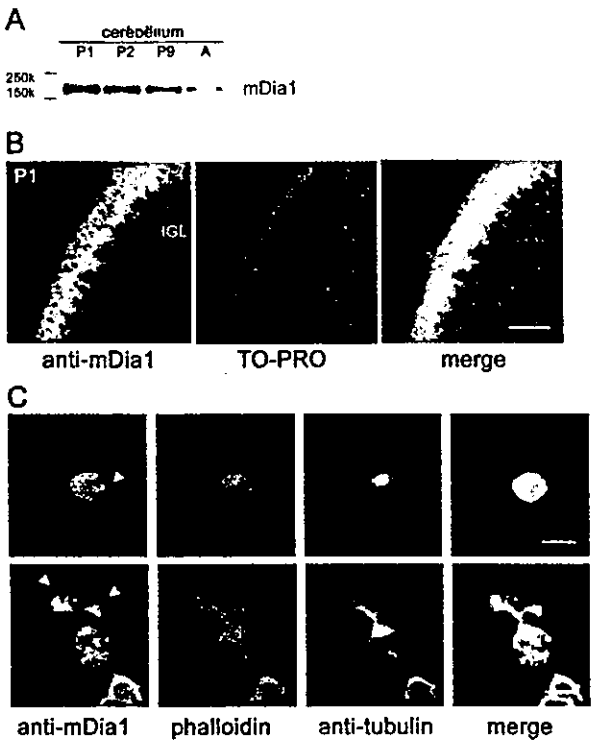

Figure 5. **High expression of mDia1 in cerebellar EGL during early postnatal development.** (A) Western blot analysis of mDia1 expression in cerebellar lysates at P1, P2, P9, or in adult (A). (B) mDia1-like immunoreactivity is highly concentrated at and beneath the EGL at P1. TO-PRO nuclear stain indicates the locations of the cells. Bar, 50 μm. (C) mDia1 is highly expressed at the neck of a nascent process (top, arrowhead) or in the growth cones (bottom, arrowheads) in cerebellar granule cells in culture at 6 h (top) and 12 h (bottom) in vitro. mDia1 heavily colocalized with F-actin (phalloidin) and microtubules (tubulin) structures. Bars, 5 μm.

To ask directly whether mDia1 activity facilitated, at least in part, axon formation and elongation in cerebellar granule neurons, we tested whether expression of the DA-mDia1 mutant was sufficient to replicate the SDF-1α–induced axon elongating activity in the absence of ROCK pathway which was blocked with Y-27632. Transfection was performed immediately after trituration and during initial plating of the neurons so that expression of exogenous protein was initiated ~6 h after plating (Bito et al., 2000, and this study). Neurons were fixed using PFA at 12 h after transfection to examine the effect of mDia1 activity on axon initiation and elongation. Indeed, mDia1-ΔN3–expressing cerebellar granule cells revealed a similar number of axons as GFP-expressing control cells; however, the axons were significantly longer compared with the mock-transfected neurons in the presence of Y-27632 (Fig. 6, A–D), consistent with the idea that mDia1 may work downstream of Rho to facilitate axon growth.

During transfection of mDia1-ΔN3, we noticed that the newly formed processes were abnormal in neurons untreated with Y-27632. Axon outgrowth seemed to be prematurely aborted as processes were filled with an exuberant amount of filamentous actin and β-tubulin (Fig. 6 B, mDia1-ΔN3), and thus exhibited an abnormal width (Fig. 6 B and unpublished data). Basal ROCK activity, in the context of excessive mDia1 activity, might account for a prominent increase in actin polymerization (Watanabe et al., 1999), while also sustaining a tonic level of actomyosin contractility, thereby negatively acting on axon elongation.

Rho/mDia pathway mediates SDF-1α–stimulated axon elongation in cerebellar granule neurons in part via a coordination with a Rac-dependent pathway

We next examined the contribution of endogenous mDia1 on SDF-1α–stimulated axon elongation by use of a dominant-negative (DN) form of mDia1, mDia1-ΔN3(HindIII) (Fig. 4 A; Tsuji et al., 2002). This mutant was able to abolish the effect of DA-mDia1 on axon length (Fig. 7 A). DN-mDia1 also inhibited axon numbers back to baseline levels (Fig. 7 A); however, since DA-mDia1 had little effect per se (Fig. 6 D), we currently favor the simplest view that rather than acting on the axonogenesis itself, mDia's axon elongating activity may be required in order to visualize even the smallest process. Consistently, when this DN mutant was transfected in neurons stimulated with SDF-1α in the presence of Y-27632, both axon number and axon length were significantly diminished (Fig. 7, B and C). Together, these results support the notion that axon elongation induced by SDF-1α may be regulated in an mDia-dependent manner.

To obtain an independent confirmation of these results, we applied the RNA interference techniques using short interfering double stranded RNA oligomers (siRNAs) (Elbashir et al., 2001). mDia1-specific siRNA was designed and its efficiency in knocking down mDia1 protein was tested in NIH3T3 cells by Western blot analysis (Fig. 8 A). Loss of mDia1 immunoreactivity was specifically obtained in cells expressing a cotransfection marker enhanced GFP (EGFP; unpublished data). Using identical transfection procedures, EGFP-positive cerebellar granule neurons were screened to identify the neurons, which have taken up the mDia1 siRNA, and axon lengths were measured in these neurons. A significant reduction was observed both in axon numbers and in axon length (Fig. 8, B and C), compared with scramble siRNA-treated neurons, in keeping with the DN approach.

We finally wanted to examine the relevance of mDia1 activity vis-a-vis of Rac, a small GTPase classically found to mediate axon outgrowth. A DN form of Rac, RacN17, was introduced into cerebellar granule cells along with a DA-mDia1 mutant mDia1-ΔN3. Axon elongation facilitated by DA-mDia1 in the presence of Y-27632 was repressed, in the presence of RacN17, back to baseline levels (Fig. 9 A). These findings are most consistent with the idea that Rac may significantly contribute to the mDia effect on axon outgrowth. Thus, mDia may directly regulate Rac or one of its upstream regulators.

Could Rho/mDia pathway regulate Rac? We recently proposed a candidate mechanism in HeLa and Swiss3T3 cells: as ROCK is known to down-regulate Rac activity, ROCK inhibition, under some circumstances, may suffice to up-regulate Rac via mDia1 (Tsuji et al., 2002). We tested whether such a possibility may be true in cerebellar granule

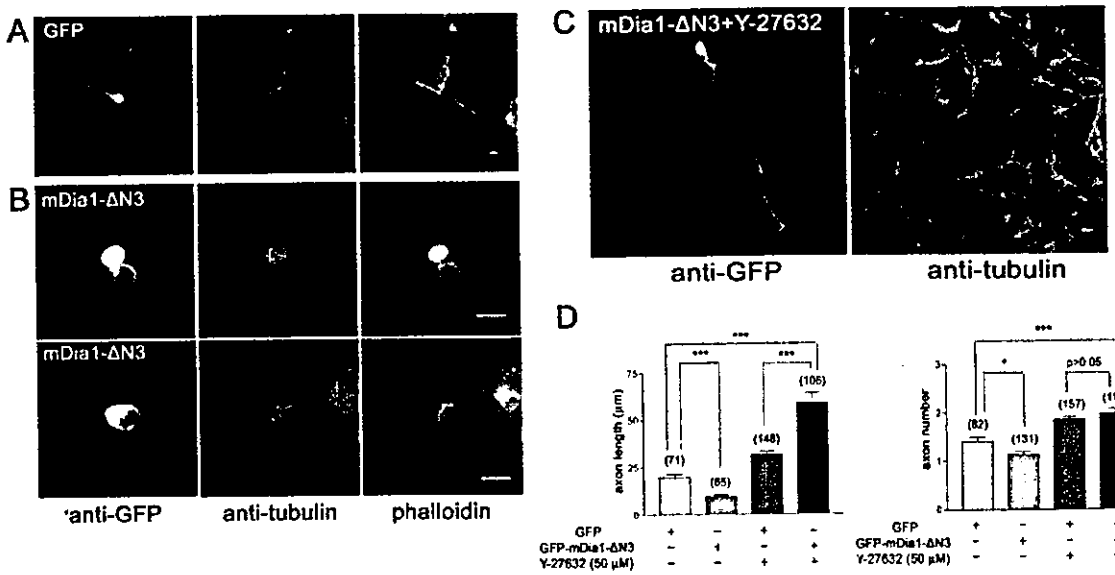

Figure 6. **DA mDia1 facilitates axon elongation.** Morphology of cerebellar granule cells overexpressing GFP (A), GFP-mDia1-ΔN3 alone (B), or GFP-mDia1-ΔN3 in the presence of Y-27632 (C). When ROCK activity was reduced, expression of GFP-mDia1-ΔN3 resulted in a significantly enhanced elongation (D, left) of axons ($n \approx 65$–157) compared with EGFP-expressing controls (A). Overexpression of GFP-mDia1-ΔN3 alone successfully induced an axon, which, however, exhibited a significantly altered shape (enlarged width, premature stop), presumably due to an increased actin stability in the presence of intact ROCK activity (B). Basal ROCK activity, in the context of excessive mDia1 activity, might cause a prominent increase in actin polymerization, while also sustaining a tonic level of actomyosin contractility, thereby negatively acting on axon elongation. *$P < 0.05$; ***$P < 0.001$. Bars, 5 μm.

Figure 7. **A DN mDia1 mutant interferes with SDF-1α–dependent axon elongation.** (A) Coexpression of the GFP-mDia1-ΔN3(HindIII) mutant abolished the effect of FLAG-mDia1-ΔN3 expression on axon length (left). $n \approx 33$–80. (B and C) The effect of GFP-mDia1-ΔN3(HindIII) overexpression was examined on SDF-1α–facilitated axon elongation in the presence of Y-27632. A potent inhibition on both SDF-1α–dependent axon elongation (B and C, left) and axon initiation (B and C, right) was detected. $n \approx 35$–145. Bars, 5 μm.

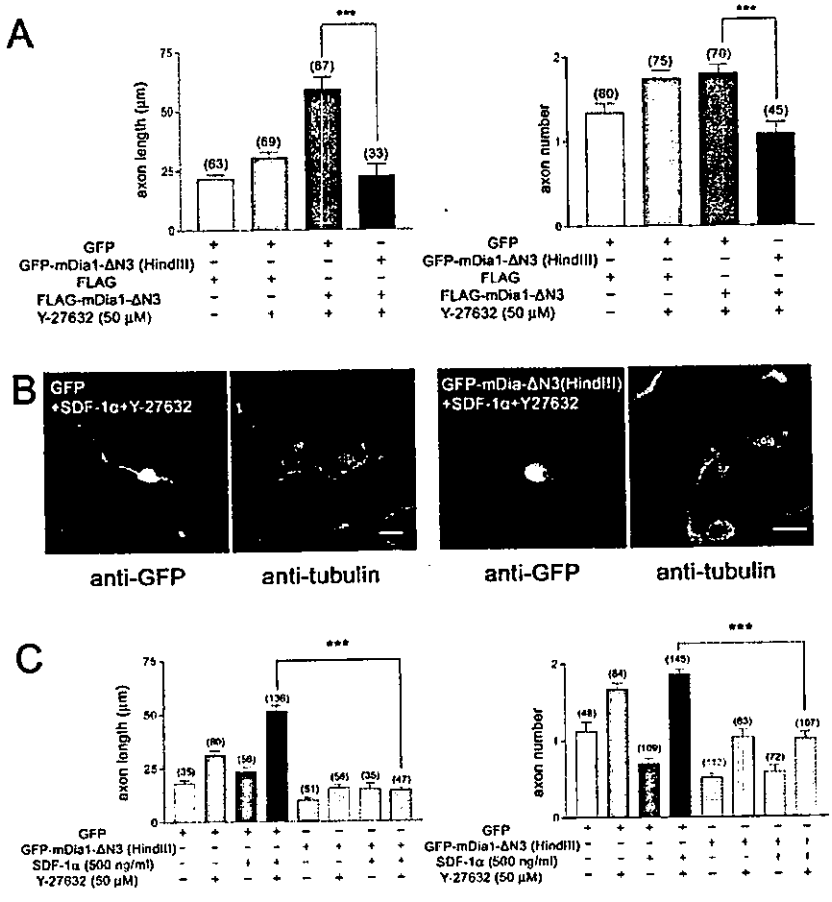

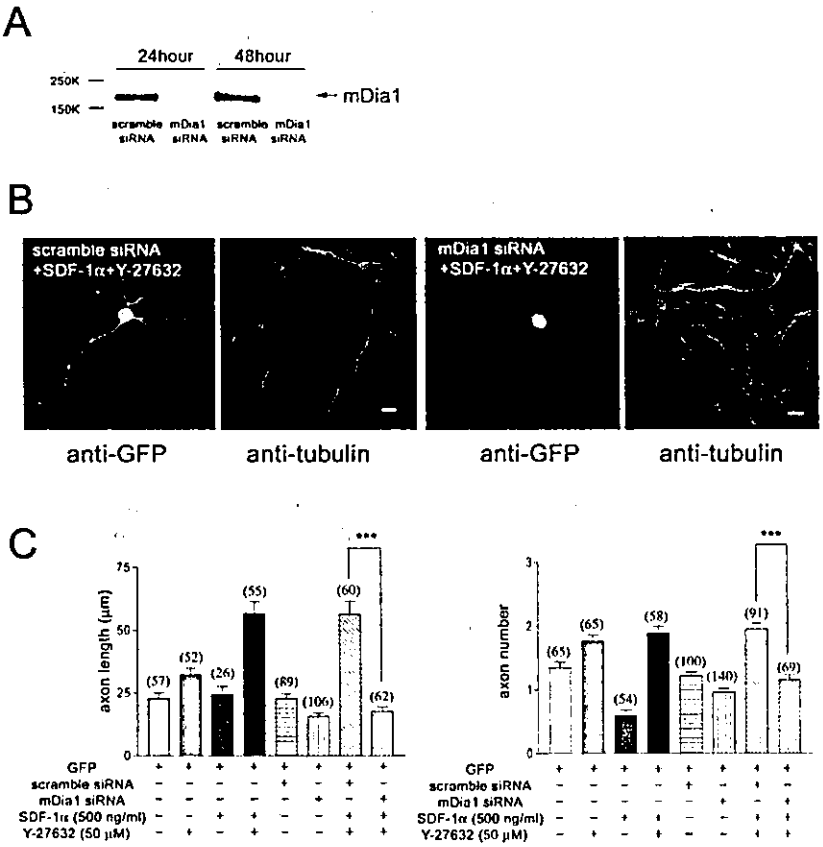

Figure 8. **mDia1 knockdown by RNAi using siRNA completely abolishes SDF-1α–dependent axon elongation.** (A) Significant reduction of mDia1 protein is achieved in NIH3T3 within 24 h by RNAi using siRNA. (B and C) mDia1 knockdown by RNAi annihilates both SDF-1α–dependent axon elongation (C, left) and axon initiation (C, right) back to baseline levels, thereby confirming the DN experiments. $n \approx 26$–140. ***$P < 0.001$. Bars, 5 μm.

cells. Consistent with previous work, Y-27632 treatment in SDF-1α–stimulated neurons was sufficient to increase the GTP-bound form of Rac (Fig. 9 B).

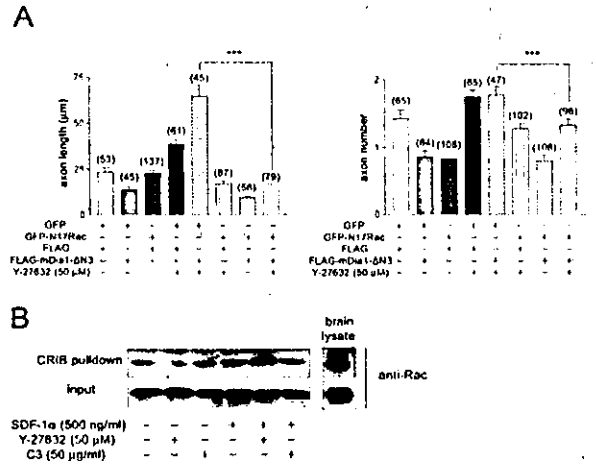

Figure 9. **Expression of the morphological effects of mDia1 is mediated, at least in part, by Rac activity.** (A) Co-expression of GFP-N17Rac, a DN mutant of Rac, suppresses expression of the facilitatory effects of FLAG-mDia1-ΔN3 on either axon length (left) in the presence of Y-27632 (50 μM) back to baseline levels. $n \approx 45$–137. (B) Inhibition of ROCK activity in the presence of high concentration of SDF-1α (500 ng/ml) increases the GTP-bound form of Rac. ***$P < 0.001$.

Together, our data establish a critical role for the Rho/mDia1 pathway in mediating axon elongation in SDF-1α–stimulated cerebellar granule neurons, presumably in concert with Rac activity (Fig. 10).

Discussion

Discovery of a Rho/mDia-dependent signaling pathway crucial for axon elongation

Previous reports have shown an antagonism between Rac- and Rho-mediated pathways in neurite extension and control of axonal growth cones (for review see Narumiya et al., 1997; Gallo and Letourneau, 1998; Hall, 1998; Luo, 2000; Dickson, 2001; Nikolic, 2002). In the mammalian CNS, we showed that enhanced Rho/ROCK activity led to inhibition of axonogenesis, whereas inhibition of Rho/ROCK pathway induced precocious outgrowth of neurites (Bito et al., 2000). In spite of a few reports suggesting a distinct, rather facilitatory effect for Rho during neuritogenesis (Threadgill et al., 1997; Sebok et al., 1999; Bashaw et al., 2001), it has remained unclear whether these experimental results truly reflected a genuine primary effect mediated by Rho.

In this study, we have formally demonstrated that Rho may in fact mediate both stimulation and inhibition of axon outgrowth downstream of the same ligand SDF-1α in the context of early postnatal cerebellar granule cells. Although a classically recognized Rho/ROCK pathway repressed axon formation, a Rho/mDia pathway was identified which rather potently facilitated axon elongation. How ROCK can domi-

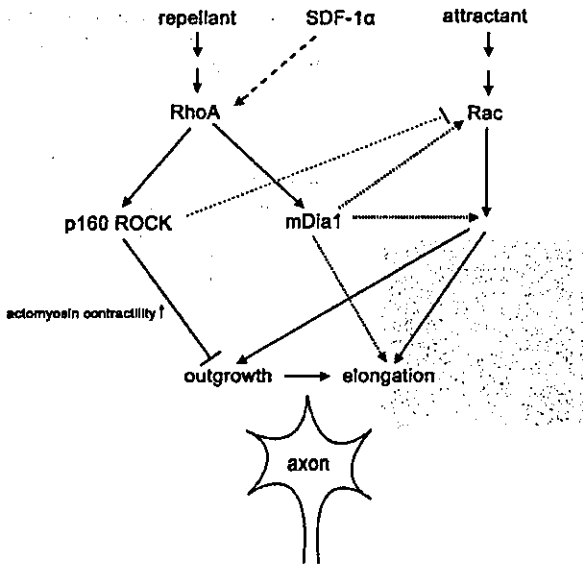

Figure 10. **Proposed model for the role of mDia in SDF-1α–dependent axon outgrowth in cultured cerebellar granule neurons.** Usually Rho and Rac antagonistically controls axon outgrowth. During the very early stages in the primary culture, ROCK action predominates to favor suppression of precocious outgrowth of axons from the cerebellar granule cells. However, as these neurons express a high amount of mDia1 gradual decline in ROCK activity facilitates expression of Rho-dependent mDia1 activity and a subsequent recruitment of a signaling complex, which in concert with the Rac-dependent signaling cascade may help the transition from inhibition to stimulation of axon outgrowth and elongation. Thus, the SDF-1α/Rho/mDia1 pathway may play a critical role in defining and modulating the balance between the Rho- and Rac-based signaling pathways during axon outgrowth.

nantly antagonize the expression of the axon elongation machinery, while another Rho effector mDia is facilitating this event, is currently being investigated. One possibility that is consistent with our finding is that ROCK and mDia1 may locally respond to different levels of GTP-bound Rho. Our finding of a multiplicity in Rho-mediated sites of action is reminiscent of the recent findings suggesting that Rac also acts on multiple steps of axon outgrowth during *Drosophila* development (Ng et al., 2002).

How then does mDia, an adaptor protein containing multiple formin homology domains, exert its effect on axon elongation? A clear picture is still missing, since only a few binding partners of mDia such as profilin (Watanabe et al., 1997), IRSp53 (Fujiwara et al., 2000), or mDia-interacting protein (Satoh and Tominaga, 2002) have been reported. Interestingly, in *Saccharomyces cerevisiae* the Diaphanous homologue Bni1p was shown to be critically involved in controlling assembly of actin cables required for establishment of cell polarity and directed growth (Ozaki-Kuroda et al., 2001; Pruyne et al., 2002; Sagot et al., 2002). Furthermore, recently a DA mutant of mDia1 was also shown to affect orientation of microtubules in HeLa cells, thus implying that mDia may perhaps spatially coordinate actin polymerization and the stability/rate of assembly of microtubule polymers (Ishizaki et al., 2001; Palazzo et al., 2001).

Intriguingly, in our study Rac activity was shown to be required to support an mDia-based change in neuronal morphology. Indeed, a high amount of basal Rac activity is found in the early postnatal cerebellum (unpublished data). In vivo and in vitro studies examining the consequence of defects in Rac/Pak/Cdk5/p35 signaling have provided numerous lines of evidence in support for a role for Rac-mediated control of cytoskeletal dynamics during axon outgrowth (Luo et al., 1994, 1996; Nikolic et al., 1996, 1998; Kaufmann et al., 1998; Hing et al., 1999; Newsome et al., 2000; Zukerberg et al., 2000; Ng et al., 2002). Since we detected an increase in Rho but not Rac activity upon SDF-1α stimulation, we presume that Rac may play a rather permissive role in mediating the Rho/mDia-dependent events, although we cannot exclude the possibility that mDia may also directly regulate Rac or one of its upstream regulators (Fig. 9; Tsuji et al., 2002).

A critical role for a pial chemokine SDF-1α as a guidance molecule regulating axon outgrowth

Recently, SDF-1α (Tashiro et al., 1993; Nagasawa et al., 1994) has attracted a lot of attention as a prototypical chemokine that acts as a mitogen and participates in positional control of a large variety of highly differentiated cell types. Gene targeting of either the ligand molecule SDF-1α or its receptor CXCR4 resulted in a strikingly similar phenotype in the respective knockout mice, thereby demonstrating a crucial role for SDF-1α/CXCR4 signaling in the development of appropriate cell layer formation in the cerebellum, the hippocampal dentate gyrus, the thymus, the spleen, vascular endothelium, and the intestinal epithelium (Nagasawa et al., 1996; Ma et al., 1998; Tachibana et al., 1998; Zou et al., 1998; Lu et al., 2002). In the cerebellum, absence of SDF-1α/CXCR4 signaling resulted in premature invasion of many proliferating granule cells into the cerebellar anlage, and aberrant onset of migration from the external granule cell layer (EGL) to the internal granule cell layer (IGL) (Ma et al., 1998; Zou et al., 1998). Complementary experiments demonstrated that SDF-1α acted as a chemoattractant for migration of both EGL- and IGL-derived cerebellar granule cells in culture (Klein et al., 2001; Lu et al., 2001; Zhu et al., 2002). Together, these lines of evidence are consistent with the idea that neuronal migration and patterning may heavily involve chemokine and G protein–coupled receptor signaling.

However, it was not known which exact step of neuronal morphogenesis was directly targeted by SDF-1α, nor was it clear what intracellular signaling it activated in order to fulfill its role as a neural guidance molecule. Here we found that a large part of the initial morphogenetic and cytoskeletal action of SDF-1α might be specifically mediated by the Rho signaling pathway, independent of its potency as a mitogen, in a pertussis toxin-insensitive manner (unpublished data). Previously, it was suspected that SDF-1α might exhibit its growth promoting or chemotactic effect on neurons via pertussis-sensitive Gi/o heterotrimeric G proteins (Klein et al., 2001) and/or via PLC-mediated activation of intracellular calcium stores (Klein et al., 2001; Lu et al., 2002). The possible contribution of these signaling pathways to the neurite elongation still needs to be properly addressed in our cultured cerebellar granule neurons.

Control of actin dynamics via multiple effectors of small GTPases: potential antagonism and coordination between distinct signaling pathways

Our study demonstrates that the Rho-dependent signaling cascade implicated in the developmental control of neural hardwiring may consist of two apparently opposing streams of signals: an inhibitory pathway mediated by ROCK (Bito et al., 2000) and a facilitatory pathway mediated by mDia1 (this study). Coordination of these two pathways may be suited to sequentially express the unique property of SDF-1α either as a repellant or as an attractant. These findings shed light on the new possibility that Rho- and Rac-dependent pathways may interact not just in an antagonistic but also in a cooperative way in the regulation of the timing and the extent of axon elongation in cultured cerebellar granule cells (Fig. 10). Our study raises the possibility that the stimulation of Rho/mDia-mediated pathway by SDF-1α might provide a modulatory link between the Rho- and Rac-based modes.

Together, these findings underscore the significance of ROCK/mDia antagonism during early CNS development. An appropriate balance and coordination between these two signaling systems may be key to controlling the initial timing and extent of axon outgrowth as a function of the strength of stimuli exhibited by the gradient of external guidance cues such as the pial chemokine SDF-1α.

Materials and methods

Primary culture of mouse cerebellar granule cells

Mouse cerebellar granule cell cultures were as described in Bito et al. (2000). A detailed protocol can be obtained from the authors upon request.

Materials and reagents

Y-27632, a ROCK inhibitor, was supplied by Dr. Masayoshi Uehata (Mitsubishi Pharma Co., Osaka, Japan). Botulinum C3 exoenzyme was purified as described (Morii and Narumiya, 1995). SDF-1α was purchased from PeproTech EC. GST-Rhotekin RBD and GST-PAK CRIB proteins were prepared as described (Ren et al., 1999; Tsuji et al., 2002). pEGFP-C1 was from CLONTECH Laboratories, Inc. pEGFP-mDia1ΔN3, pFL-mDia1ΔN3, pEGFP-mDia1ΔN3 (HindIII), and pEGFP-N17Rac were as described (Watanabe et al., 1999; Tsuji et al., 2002). All other reagents were of analytical grade unless noted otherwise.

Transient transfection of plasmid cDNA constructs and pharmacological assays

Transfection was performed in the following way as modified from Bito et al. (2000). At the end of cerebellar granule cell preparation, a cell pellet was recovered from a 1,000 rpm, 10-min centrifugation at 4°C and resuspended with 20% FCS/HANKS(−) at densities of 5×10^5 cells. The cell mixture (80 μl) was plated onto 12-mm round Matrigel-coated (Becton Dickinson) coverslips (Assistent) placed in a 24-well plate. Each coverslip had been coated with 80 μl Matrigel, 4 h before use. Cells were allowed to settle down for 30 min at RT and were incubated for 30 min at 37°C in a CO_2 incubator after each coverslip was fed with 0.5 ml of Medium A (Earle's MEM supplemented with 10% FCS [Hyclone], 1× B-27 supplement [Invitrogen], insulin [25 mg/L; Sigma-Aldrich], glucose [5 g/L], transferrin [100 mg/L; Calbiochem], and 2 mM glutamine). Then, for each coverslip subjected to transfection 100 μl OptiMEM (Invitrogen) containing a total amount of 1 μg of plasmids (0.5 μg of each plasmid for cotransfection) and 1 μl of Lipofectamine 2000 (Invitrogen) was added drop by drop. The plate was incubated in a CO_2 incubator for 3 h and replaced with 0.5 ml of Medium A (same as above) per well. When necessary, either Rho or ROCK activity was inhibited in transfected cells by adding Y-27632 (final concentration 50 μM) or C3 (final concentration 50 μg/ml), respectively. Cells were put back into a CO_2 incubator and cultured for another 12 h.

To examine the effect of various pharmacological reagents on various aspects of axon outgrowth, cerebellar granule cells were plated onto 12-mm round Matrigel-coated coverslips placed in a 24-well plate as described above. Cells were allowed to settle down for 30 min at RT. After each coverslip was fed with 0.5 ml of Medium A, they were incubated for another 3.5 h at 37°C in a CO_2 incubator and then replaced with Medium A supplemented with either the vehicle or SDF-1α (500 ng/ml), Y-27632 (50 μM), SDF-1α (10, 100, 250, 500, and 1,000 ng/ml) plus Y-27632 (50 μM), SDF-1α (500 ng/ml) plus C3 (50 μg/ml), and indicated concentrations of C3 exoenzyme. The cells were put back into a CO_2 incubator and cultured for another 12 h.

Pharmacological assays were performed in transfected cells in a similar way except that the cells were incubated in a CO_2 incubator for 3 h after the end of transfection procedure and then replaced with 0.5 ml of Medium A containing similar amounts of drugs as described above.

For transfection, Swiss-3T3 cells were plated on a cover glass at a density of 2×10^4 cells per 22-mm dish and cultured in DME containing 10% FCS for 24 h. The cells were washed with PBS(−) once and incubated with the indicated amounts of pEGFP-C1 or pEGFP-mDia1-ΔN3 mixed with 1 μl of Lipofectamine 2000 for 3 h in 1 ml of OPTI-MEM. The medium was replaced with DME containing 10% FCS, and the cells were cultured for 18 h. The cells were then cultured in serum-free DME for 24 h and treated with 30 μM Y-27632 for the last 30 min. The cells were fixed and stained as described below.

Immunofluorescence microscopy and measurements of axon parameters

Immunocytochemistry and GFP-imaging was performed essentially as described (Bito et al., 1996, 2000) using a LSM 510 system (Carl Zeiss MicroImaging, Inc.). Primary and secondary antibodies were as follows: rabbit polyclonal anti-p140mDia1 antibody (AP50) (Watanabe et al., 1997), anti-FLAG mAb (M2; Eastman Kodak Co.), rat antitubulin mAb (Chemicon), anti–β-tubulin mAb (TUB.2.1) (Sigma-Aldrich); anti-GFP monoclonal and polyclonal (Molecular Probes); and Alexa Fluor 488–, 594–, and 633–conjugated goat anti–rabbit, anti–rat, and anti–mouse secondary (Molecular Probes). Alexa Fluor 594–, and 633–phalloidin (1:1,000; Molecular Probes) were used to stain the F-actin. In all image analyses, no background subtraction was performed, and all pseudocolor representations were assembled using Adobe Photoshop® version 6.0 for illustrative purpose only.

Quantitation of axon length and number was performed on cerebellar granule neurons cultured in the presence of 10% FCS using parameters similar to those described previously (Bito et al., 2000). Axons were distinguished from the filopodia by the presence of microtubules as verified by β-tubulin staining. As established previously (Bito et al., 2000), β-tubulin immunoreactivity was missing in virtually all processes with less than 3 μm in length. Because the average axon number was below two (i.e., exact number was usually one or zero) during the experimental time window in most of our assays in this study, we restricted our measurement of axon length to the longer first process. Since an axon was equal or larger than 3 μm in length, its contour could be unambiguously traced from the cell soma up to the very tip of the processes; all turning points within the longest process was defined and the sum of the cumulated distances between these points was considered as axon length. The calculation was performed off-line using the software plug-in of the LSM 510 system. Measurements in transfected neurons were performed identically except that transfected neurons were first identified using an antitag immunostaining (with an anti-GFP or an anti-FLAG antibody) to maximize the probability of detection; when directly compared, FLAG- and GFP-tagged constructs yielded similar results and phenotypes. Statistical analyses were performed using Prism 3.02 (Graphpad Software). All data are indicated as means ± SEM. Unpaired *t* test with Welch's correction was employed to determine statistical significance and p values below 0.05 was considered as significant.

Videomicroscopy

Cerebellar granule cells labeled with PKH-26 (Sigma-Aldrich) were seeded at a density of 10^5 per dish in a 35-mm glass-bottom dish (Matsunami Glass) and cultured for 3 h. The dish was transferred to a temperature-controlled CO_2 incubator (Carl Zeiss MicroImaging, Inc.) attached to the microscope stage. SDF-1α (100 ng/ml, a final concentration) was then added, and the cell movement was monitored at 37°C in 5% CO_2 for 60 min using a confocal laser scanning unit (LSM 510-V2.5; Carl Zeiss MicroImaging, Inc.). One optical section was acquired every 3 min, and the video image were constructed from these sequential images.

Immunohistochemistry

P1 or adult brain was taken out and immediately frozen in TissueTek O.C.T. Compound (Sakura) on dry ice. Cryostat sections of 20-μm width were obtained and subjected to indirect immunofluorescence staining using an anti-p140mDia1 primary (AP50; Watanabe et al., 1997) and Alexa

Fluor 488–conjugated goat anti–rabbit secondary antibodies. TO-PRO-3 iodide (Molecular Probes) was used for nuclear staining. Specimens were examined on Axioplan or LSM 510 confocal imaging system (Carl Zeiss MicroImaging, Inc.). Stacked optical sections were merged using Maximum Projection Software (Carl Zeiss MicroImaging, Inc.).

Western blot analysis

Total brain or cerebellar tissues were collected from ICR mice of indicated ages. Thin slices were cut in parasagittal directions in ice-cold HANKS and lysed in the lysis buffer containing 50 mM Tris-HCl, pH 7.5, 150 mM NaCl, 1% NP-40, 0.5% sodium deoxycholate, and 1× Complete (Protease Inhibitor Cocktail Tablets) (Roche Diagnostics). The samples were centrifuged at 100,000 *g* for 30 min, and the supernatant was collected as the cell lysates. Protein concentration of the lysates was determined by the Lowry method. For Western blot analysis using the total cell lysates, one fifth volume of the 5× Laemmli sample buffer was added to the lysates. The mixtures were boiled for 5 min and subjected to SDS-PAGE and Western blot analysis using anti-p140mDia1 antibody (AP50).

Rho and Rac pull-down assays

Cerebellar granule cells were plated at a density of 5×10^5 cells per 10-cm dish. After treatment with Y-27632, C3 exoenzyme, and/or SDF-1α, the cells were washed once with ice-cold HANKS and lysed in the pull-down lysis buffer containing 50 mM Tris-HCl, pH 7.5, 100 mM NaCl, 2 mM $MgCl_2$, 10% glycerol, 1% NP-40, 1× Complete (Roche Diagnostics), 1 mM sodium fluoride, 1 mM EGTA, and 1 mM PMSF. The samples were centrifuged at 12,000 *g* for 30 min, and the supernatants were saved as the cell lysates. For cerebellar tissue lysates, cerebella were collected from P1 and adult ICR mice, and thin slices were cut in parasagittal directions in ice-cold HANKS and lysed in the pull-down lysis buffer. The tissue lysates were centrifuged at 100,000 *g* for 30 min, and the supernatant was collected as the cell lysates. 200 μg of cell lysates was incubated with 20 μg GST-Rhotekin RBD or GST-PAK CRIB immobilized on glutathione–Sepharose 4B beads (Amersham Biosciences) for 1 h at 4°C. Beads were washed three times with the pull-down buffer, and GTP-bound RhoA and GTP-bound Rac1 were detected by Western blot with an anti-RhoA (Santa Cruz Biotechnology, Inc.) and an anti-Rac1 antibody (Upstate Biotechnology). Protein concentration was determined by the Lowry method.

Protein knockdown of mDia1 by RNAi using siRNA

siRNA corresponding to mDia1 mRNA sequences were designed as recommended with 5′-phosphate, 3′-hydroxyl, and two-base overhangs on each strand; it was chemically synthesized and annealed for duplex siRNA formation by Dharmacon Research, Inc. The following gene-specific sequences were used successfully: si-mDia1 (K2) sense 5′-GCUGGUCAGAGCCAUGGAU-3′ and antisense 5′-CGACCAGUCUCGGUACCU-3′. Transfection of mDia1 siRNA for NIH-3T3 cells (10^4 cells/ml) was performed with Lipofectamine 2000 in 6-well plates. Per well, 2 μl lipofectamine 2000 diluted in 100 μl Opti-MEM was applied to a premix consisting of siRNA (20 μM, 4 μl)/Opti-MEM (100 μl) and incubated for 30 min. The whole mixture was added to the medium, which then was changed to DME 3 h after transfection. Cells were incubated for 24–48 h before analysis of knock-down mDia1 by Western blot as described above.

Cotransfection of pEGFP-C1 and siRNA to cerebellar granule cells (5×10^5 cells/ml) were performed with Lipofectamine 2000. Briefly, for 10^6 cells 2 μl Lipofectamine 2000 diluted in 100 μl Opti-MEM was applied to a pEGFP-C1 (1 μg)/siRNA (20 μM, 8 μl)/Opti-MEM (200 μl) mixture and incubated for 30 min. The entire mixture was then added to the cell-containing medium, which was refed with the original culture medium 3 h after transfection. Cells were incubated for 12 h in solution and then finally plated onto 12-mm round Matrigel-coated coverslips placed in a 24-well plate. After another 12 h of culture on the coverslips, measurements of axon parameters were performed as described above.

Online supplemental material

Video 1, showing facilitation of axon elongation by a 100 ng/ml SDF-1α treatment in cultured cerebellar granule neurons, is available online at http://www.jcb.org/cgi/content/full/jcb.200210149/DC1).

We thank K. Nonomura, H. Nose, and T. Arai for assistance, T. Ishizaki and N. Watanabe for discussion, and S. Arakawa for support.

This work was supported in part by grants in aid from the Ministry of Education, Culture, Sports, Science and Technology of Japan (to S. Narumiya, K. Kimura, and H. Bito) and grants from PRESTO-Japan Science and Technology Corporation, the Tanabe Medical Frontier Conference, the Cell Science Research Foundation, and Human Frontier Science Program (to H. Bito). T. Furuyashiki is a postdoctoral fellow and Y. Arakawa and S. Takemoto-Kimura are predoctoral fellows from the Japan Society for Promotion of Science.

Submitted: 28 October 2002
Revised: 10 March 2003
Accepted: 10 March 2003

References

Altman, J., and S.A. Bayer. 1996. The third stage of cerebellar development: maturation of the cerebellar system. *In* Development of the Cerebellar System. CRC Press, Boca Raton, FL. 324–469.

Bashaw, G.J., H. Hu, C.D. Nobes, and C.S. Goodman. 2001. A novel Dbl family RhoGEF promotes Rho-dependent axon attraction to the central nervous system midline in *Drosophila* and overcomes Robo repulsion. *J. Cell Biol.* 155:1117–1122.

Bhatt, R.S., T. Tomoda, Y. Fang, and M.E. Hatten. 2000. Discoidin domain receptor 1 functions in axon extension of cerebellar granule neurons. *Genes Dev.* 14:2216–2228.

Bito, H., K. Deisseroth, and R.W. Tsien. 1996. CREB phosphorylation and dephosphorylation: a Ca^{2+}- and stimulus duration-dependent switch for hippocampal gene expression. *Cell.* 87:1203–1214.

Bito, H., T. Furuyashiki, H. Ishihara, Y. Shibasaki, K. Ohashi, K. Mizuno, M. Maekawa, M. Ishizaki, and S. Narumiya. 2000. A critical role for a Rho-associated kinase, p160ROCK, in determining axon outgrowth in mammalian CNS neurons. *Neuron.* 26:431–441.

Dickson, B.J. 2001. Rho GTPases in growth cone guidance. *Curr. Opin. Neurobiol.* 11:103–110.

Driessens, M.H., H. Hu, C.D. Nobes, A. Self, I. Jordens, C.S. Goodman, and A. Hall. 2001. Plexin-B semaphorin receptors interact directly with active Rac and regulate the actin cytoskeleton by activating Rho. *Curr. Biol.* 11:339–344.

Elbashir, S.M., J. Harborth, W. Lendeckel, A. Yalcin, K. Weber, and T. Tuschl. 2001. Duplexes of 21-nucleotide RNAs mediate RNA interference in cultured mammalian cells. *Nature.* 411:494–498.

Fujiwara, T., A. Mammoto, Y. Kim, and Y. Takai. 2000. Rho small G-protein-dependent binding of mDia to an Src homology 3 domain-containing IRSp53/BAIAP2. *Biochem. Biophys. Res. Commun.* 271:626–629.

Gallo, G., and P.C. Letourneau. 1998. Axon guidance: GTPases help axons reach their targets. *Curr. Biol.* 8:R80–R82.

Goodman, C.S., and C.J. Shatz. 1993. Developmental mechanisms that generate precise patterns of neuronal connectivity. *Cell.* 72:77–98.

Hall, A. 1998. Rho GTPases and the actin cytoskeleton. *Science.* 279:509–514.

Hatten, M.E. 1999. Central nervous system neuronal migration. *Annu. Rev. Neurosci.* 22:511–539.

Hing, H., J. Xiao, N. Harden, L. Lim, and S.L. Zipursky. 1999. Pak functions downstream of Dock to regulate photoreceptor axon guidance in *Drosophila*. *Cell.* 97:853–863.

Huang, E.J., and L.F. Reichardt. 2001. Neurotrophins: roles in neuronal development and function. *Annu. Rev. Neurosci.* 24:677–736.

Ishizaki, T., M. Uehata, I. Tamechika, J. Keel, K. Nonomura, M. Maekawa, and S. Narumiya. 2000. Pharmacological properties of Y-27632, a specific inhibitor of rho-associated kinases. *Mol. Pharmacol.* 57:976–983.

Ishizaki, T., Y. Morishima, M. Okamoto, T. Furuyashiki, T. Kato, and S. Narumiya. 2001. Coordination of microtubules and the actin cytoskeleton by the Rho effector mDia1. *Nat. Cell Biol.* 3:8–14.

Jin, Z., and S.M. Strittmatter. 1997. Rac1 mediates collapsin-1-induced growth cone collapse. *J. Neurosci.* 17:6256–6263.

Jurney, W.M., G. Gallo, P.C. Letourneau, and S.C. McLoon. 2002. Rac1-mediated endocytosis during Ephrin-A2- and Semaphorin 3A-induced growth cone collapse. *J. Neurosci.* 22:6019–6028.

Kaufmann, N., Z.P. Wills, and D. Van Vactor. 1998. *Drosophila* Rac1 controls motor axon guidance. *Development.* 125:453–461.

Klein, R.S., J.B. Rubin, H.D. Gibson, E.N. DeHaan, X. Alvarez-Hernandez, R.A. Segal, and A.D. Luster. 2001. SDF-1 alpha induces chemotaxis and enhances Sonic hedgehog-induced proliferation of cerebellar granule cells. *Development.* 128:1971–1981.

Li, X., E. Saint-Cyr-Proulx, K. Aktories, and N. Lamarche-Vane. 2002. Rac1 and Cdc42 but not RhoA or Rho kinase activities are required for neurite outgrowthInduced by the Netrin-1 receptor DCC (deleted in colorectal cancer) in N1E-115 neuroblastoma cells. *J. Biol. Chem.* 277:15207–15214.

Liu, B.P., and S.M. Strittmatter. 2001. Semaphorin-mediated axonal guidance via Rho-related G proteins. *Curr. Opin. Cell Biol.* 13:619–626.

Lu, M., E.A. Grove, and R.J. Miller. 2002. Abnormal development of the hippocampal dentate gyrus in mice lacking the CXCR4 chemokine receptor. *Proc. Natl. Acad. Sci. USA.* 99:7090–7095.

Lu, Q., E.E. Sun, R.S. Klein, and J.G. Flanagan. 2001. Ephrin-B reverse signaling is mediated by a novel PDZ-RGS protein and selectively inhibits G protein-coupled chemoattraction. *Cell.* 105:69–79.

Luo, L. 2000. Rho GTPases in neuronal morphogenesis. *Nat. Rev. Neurosci.* 1:173–180.

Luo, L., Y.J. Liao, L.Y. Jan, and Y.N. Jan. 1994. Distinct morphogenetic functions of similar small GTPases: *Drosophila* Drac1 is involved in axonal outgrowth and myoblast fusion. *Genes Dev.* 8:1787–1802.

Luo, L., T.K. Hensch, L. Ackerman, S. Barbel, L.Y. Jan, and Y.N. Jan. 1996. Differential effects of the Rac GTPase on Purkinje cell axons and dendritic trunks and spines. *Nature.* 379:837–840.

Ma, Q., D. Jones, P.R. Borghesani, R.A. Segal, T. Nagasawa, T. Kishimoto, and R.T. Bronson. 1998. Impaired B-lymphopoiesis, myelopoiesis, and derailed cerebellar neuron migration in CXCR4- and SDF-1-deficient mice. *Proc. Natl. Acad. Sci. USA.* 95:9448–9453.

Morii, N., and S. Narumiya. 1995. Preparation of native and recombinant *Clostridium botulinum* C3 ADP-ribosyltransferase and identification of Rho proteins by ADP-ribosylation. *Methods Enzymol.* 256:196–206.

Nagasawa, T., H. Kikutani, and T. Kishimoto. 1994. Molecular cloning and structure of a pre-B-cell growth-stimulating factor. *Proc. Natl. Acad. Sci. USA.* 91:2305–2309.

Nagasawa, T., S. Hirota, K. Tachibana, N. Takakura, S. Nishikawa, Y. Kitamura, N. Yoshida, H. Kikutani, and T. Kishimoto. 1996. Defects of B-cell lymphopoiesis and bone-marrow myelopoiesis in mice lacking the CXC chemokine PBSF/SDF-1. *Nature.* 382:635–638.

Narumiya, S., T. Ishizaki, and N. Watanabe. 1997. Rho effectors and reorganization of actin cytoskeleton. *FEBS Lett.* 410:68–72.

Newsome, T.P., S. Schmidt, G. Dietzl, K. Keleman, B. Asling, A. Debant, and B.J. Dickson. 2000. Trio combines with dock to regulate Pak activity during photoreceptor axon pathfinding in *Drosophila*. *Cell.* 101:283–294.

Ng, J., T. Nardine, M. Harms, J. Tzu, A. Goldstein, Y. Sun, G. Dietzl, B.J. Dickson, and L. Luo. 2002. Rac GTPases control axon growth, guidance and branching. *Nature.* 416:442–447.

Nikolic, M. 2002. The role of Rho GTPases and associated kinases in regulating neurite outgrowth. *Int. J. Biochem. Cell Biol.* 34:731–745.

Nikolic, M., H. Dudek, Y.T. Kwon, Y.F. Ramos, and L.H. Tsai. 1996. The cdk5/p35 kinase is essential for neurite outgrowth during neuronal differentiation. *Genes Dev.* 10:816–825.

Nikolic, M., M.M. Chou, W. Lu, B.J. Mayer, and L.H. Tsai. 1998. The p35/Cdk5 kinase is a neuron-specific Rac effector that inhibits Pak1 activity. *Nature.* 395:194–198.

Nusser, N., E. Gosmanova, Y. Zheng, and G. Tigyi. 2002. NGF signals through TrkA, PI3 kinase, and Rac1 to inactivate RhoA during the initiation of neuronal differentiation of PC12 cells. *J. Biol. Chem.* 277:35840–35846.

Ozaki-Kuroda, K., Y. Yamamoto, H. Nohara, M. Kinoshita, T. Fujiwara, K. Irie, and Y. Takai. 2001. Dynamic localization and function of Bni1p at the sites of directed growth in *Saccharomyces cerevisiae*. *Mol. Cell. Biol.* 21:827–839.

Ozdinler, P.H., and R.S. Erzurumlu. 2001. Regulation of neurotrophin-induced axonal responses via Rho GTPases. *J. Comp. Neurol.* 438:377–387.

Palazzo, A.F., T.A. Cook, A.S. Alberts, and G.G. Gundersen. 2001. mDia mediates Rho-regulated formation and orientation of stable microtubules. *Nat. Cell Biol.* 3:723–729.

Powell, S.K., R.J. Rivas, E. Rodriguez-Boulan, and M.E. Hatten. 1997. Development of polarity in cerebellar granule neurons. *J. Neurobiol.* 32:223–236.

Pruyne, D., M. Evangelista, C. Yang, E. Bi, S. Zigmond, A. Bretscher, and C. Boone. 2002. Role of formins in actin assembly: nucleation and barbed-end association. *Science.* 297:612–615.

Ren, X.D., W.B. Kiosses, and M.A. Schwartz. 1999. Regulation of the small GTP-binding protein Rho by cell adhesion and the cytoskeleton. *EMBO J.* 18: 578–585.

Sagot, I., A.A. Rodal, J. Moseley, B.L. Goode, and D. Pellman. 2002. An actin nucleation mechanism mediated by Bni1 and Profilin. *Nat. Cell Biol.* 4:626–631.

Satoh, S., and T. Tominaga. 2002. mDia-interacting protein acts downstream of Rho-mDia and modifies Src activation and stress fiber formation. *J. Biol. Chem.* 276: 39290–39294.

Sebok, A., N. Nusser, B. Debreceni, Z. Guo, M.F. Santos, J. Szeberenyi, and G. Tigyi. 1999. Different roles for RhoA during neurite initiation, elongation, and regeneration in PC12 cells. *J. Neurochem.* 73:949–960.

Shamah, S.M., M.Z. Lin, J.L. Goldberg, S. Estrach, M. Sahin, L. Hu, M. Bazalakova, R.L. Neve, G. Corfas, A. Debant, and M.E. Greenberg. 2001. EphA receptors regulate growth cone dynamics through the novel guanine nucleotide exchange factor ephexin. *Cell.* 105:233–244.

Swiercz, J.M., R. Kuner, J. Behrens, and S. Offermanns. 2002. Plexin-B1 directly interacts with PDZ-RhoGEF/LARG to regulate RhoA and growth cone morphology. *Neuron.* 35:51–63.

Tachibana, K., S. Hirota, H. Iizasa, H. Yoshida, K. Kawabata, Y. Kataoka, Y. Kitamura, K. Matsushima, N. Yoshida, S. Nishikawa, et al. 1998. The chemokine receptor CXCR4 is essential for vascularization of the gastrointestinal tract. *Nature.* 393:591–594.

Tanaka, E., and J. Sabry. 1995. Making the connection: cytoskeletal rearrangements during growth cone guidance. *Cell.* 83:171–176.

Tashiro, K., H. Tada, R. Heilker, M. Shirozu, T. Nakano, and T. Honjo. 1993. Signal sequence trap: a cloning strategy for secreted proteins and type I membrane proteins. *Science.* 261:600–603.

Tessier-Lavigne, M., and C.S. Goodman. 1996. The molecular biology of axon guidance. *Science.* 274:1123–1133.

Tham, T.N., F. Lazarini, I.A. Franceschini, F. Lachapelle, A. Amara, and M. Dubois-Dalcq. 2001. Developmental pattern of expression of the alpha chemokine stromal cell-derived factor 1 in the rat central nervous system. *Eur. J. Neurosci.* 13:845–856.

Threadgill, R., K. Bobb, and A. Ghosh. 1997. Regulation of dendritic growth and remodeling by Rho, Rac, and Cdc42. *Neuron.* 19:625–634.

Tsuji, T., T. Ishizaki, M. Okamoto, C. Higashida, K. Kimura, T. Furuyashiki, Y. Arakawa, R.B. Birge, T. Nakamoto, H. Hirai, and S. Narumiya. 2002. ROCK and mDia1 antagonize in Rho-dependent Rac activation in Swiss 3T3 fibroblasts. *J. Cell Biol.* 157:819–830.

Uehata, M., T. Ishizaki, H. Satoh, T. Ono, T. Kawahara, T. Morishita, H. Tamakawa, K. Yamagami, J. Inui, M. Maekawa, and S. Narumiya. 1997. Calcium sensitization of smooth muscle mediated by a Rho-associated protein kinase in hypertension. *Nature.* 389:990–994.

Van Vactor, D., and J.G. Flanagan. 1999. The middle and the end: slit brings guidance and branching together in axon pathway selection. *Neuron.* 22:649–652.

Watanabe, N., P. Madaule, T. Reid, T. Ishizaki, G. Watanabe, A. Kakizuka, Y. Saito, K. Nakao, B.M. Jockusch, and S. Narumiya. 1997. p140mDia, a mammalian homolog of *Drosophila* diaphanous, is a target protein for Rho small GTPase and is a ligand for profilin. *EMBO J.* 16:3044–3056.

Watanabe, N., T. Kato, A. Fujita, T. Ishizaki, and S. Narumiya. 1999. Cooperation between mDia1 and ROCK in Rho-induced actin reorganization. *Nat. Cell Biol.* 1:136–143.

Winton, M.J., C.I. Dubreuil, D. Lasko, N. Leclerc, and L. McKerracher. 2002. Characterization of new cell permeable C3-like proteins that inactivate Rho and stimulate neurite outgrowth on inhibitory substrates. *J. Biol. Chem.* 277: 32820–32829.

Wong, K., X.R. Ren, Y.Z. Huang, Y. Xie, G. Liu, H. Saito, H. Tang, L. Wen, S.M. Brady-Kalnay, L. Mei, et al. 2001. Signal transduction in neuronal migration: roles of GTPase activating proteins and the small GTPase Cdc42 in the Slit-Robo pathway. *Cell.* 107:209–221.

Yacubova, E., and H. Komuro. 2002. Intrinsic program for migration of cerebellar granule cells in vitro. *J. Neurosci.* 22:5966–5981.

Yamasaki, T., K. Kawaji, K. Ono, H. Bito, T. Hirano, N. Osumi, and M. Kengaku. 2001. Pax6 regulates granule cell polarization during parallel fiber formation in the developing cerebellum. *Development.* 128:3133–3144.

Yamashita, T., K.L. Tucker, and Y.A. Barde. 1999. Neurotrophin binding to the p75 receptor modulates Rho activity and axonal outgrowth. *Neuron.* 24:585–593.

Zhu, Y., T. Yu, X.C. Zhang, T. Nagasawa, J.Y. Wu, and Y. Rao. 2002. Role of the chemokine SDF-1 as the meningeal attractant for embryonic cerebellar neurons. *Nat. Neurosci.* 5: 719–720.

Zou, Y.R., A.H. Kottmann, M. Kuroda, I. Taniuchi, and D.R. Littman. 1998. Function of the chemokine receptor CXCR4 in haematopoiesis and in cerebellar development. *Nature.* 393:595–599.

Zukerberg, L.R., G.N. Patrick, M. Nikolic, S. Humbert, C.L. Wu, L.M. Lanier, F.B. Gertler, M. Vidal, R.A. Van Etten, and L.H. Tsai. 2000. Cables links Cdk5 and c-Abl and facilitates Cdk5 tyrosine phosphorylation, kinase upregulation, and neurite outgrowth. *Neuron.* 26:633–646.

Molecular Biology of the Cell
Vol. 14, 1745–1756, May 2003

Citron Kinase, a Rho-dependent Kinase, Induces Di-phosphorylation of Regulatory Light Chain of Myosin II

Shigeko Yamashiro,*† Go Totsukawa,* Yoshihiko Yamakita,* Yasuharu Sasaki,‡ Pascal Madaule,§ Toshimaa Ishizaki,§ Shuh Narumiya,§ and Fumio Matsumura*†

*Department of Molecular Biology and Biochemistry, Rutgers University, Piscataway, New Jersey 08855; ‡Department of Pharmacology, Kitasato University, Tokyo, Japan; and §Department of Pharmacology, Kyoto University, Kyoto, Japan

Submitted July 25, 2002; Revised December 11, 2002; Accepted January 30, 2003
Monitoring Editor: Tom Pollard

Citron kinase is a Rho-effector protein kinase that is related to Rho-associated kinases of ROCK/ROK/Rho-kinase family. Both ROCK and citron kinase are suggested to play a role in cytokinesis. However, no substrates are known for citron kinase. We found that citron kinase phosphorylated regulatory light chain (MLC) of myosin II at both Ser-19 and Thr-18 in vitro. Unlike ROCK, however, citron kinase did not phosphorylate the myosin binding subunit of myosin phosphatase, indicating that it does not inhibit myosin phosphatase. We found that the expression of the kinase domain of citron kinase resulted in an increase in MLC di-phosphorylation. Furthermore, the kinase domain was able to increase di-phosphorylation and restore stress fiber assembly even when ROCK was inhibited with a specific inhibitor, Y-27632. The expression of full-length citron kinase also increased di-phosphorylation during cytokinesis. These observations suggest that citron kinase phosphorylates MLC to generate di-phosphorylated MLC in vivo. Although both mono- and di-phosphorylated MLC were found in cleavage furrows, di-phosphorylated MLC showed more constrained localization than did mono-phosphorylated MLC. Because citron kinase is localized in cleavage furrows, citron kinase may be involved in regulating di-phosphorylation of MLC during cytokinesis.

INTRODUCTION

Small GTPases of Rho family proteins act as molecular switches in various cellular processes including cell motility, cell division, and morphogenesis (Bokoch, 2000; Somlyo and Somlyo, 2000; Ridley, 2001; Settleman, 2001). Their main biological effects are mediated through the regulation and reorganization of the actin cytoskeleton. Rho-kinase/ROK/ROCK is one of the targets of RhoA and is involved in the assembly of stress fibers and focal adhesions in serum stimulated 3T3 cells (Chrzanowska-Wodnicka and Burridge, 1996; Leung *et al.*, 1996; Amano *et al.*, 1997; Ishizaki *et al.*, 1997; Nakano *et al.*, 1999; Watanabe *et al.*, 1999; Totsukawa *et al.*, 2000).

Citron is another target of activated Rho (Di Cunto *et al.*, 1998; Madaule *et al.*, 1998, 2000). There are two variants called citron-N and citron kinase, both of which are produced by the same transcription unit. Citron kinase is a longer variant of citron-N, including an amino-terminal serine/threonine kinase domain. It shares a high degree of structural homology with the ROCK (ROK/Rho-kinase), except that citron kinase has the SH3 binding and PDZ binding domains at its carboxyl-terminus. A shorter variant of citron-N is specifically expressed in the nervous system, and localized to the postsynaptic density, where it forms a stable complex with the membrane-associated guanylate kinase PSD-95 (Furuyashiki *et al.*, 1999; Zhang *et al.*, 1999). The functions of citron-N are unknown, although it has been suggested to link the Rho signaling cascades to NMDA receptor complexes.

Citron kinase has been suggested to play a role in cytokinesis (Madaule *et al.*, 1998; Di Cunto *et al.*, 2000). Narumiya and coworkers have reported that overexpression of citron

Article published online ahead of print. Mol. Biol. Cell 10.1091/mbc.E02–07–0427. Article and publication date are at www.molbiolcell.org/cgi/doi/10.1091/mbc.E02–07–0427.

† Corresponding authors. E-mail addresses: yamashiro@mbcl.rutgers.edu; matsumura@mbcl.rutgers.edu.

Abbreviations used: MBS, myosin binding subunit or myosin targeting subunit of myosin phosphatase; MLC, regulatory light chain of myosin II; ROCK, Rho-associated kinase, Rho-kinase or ROK.

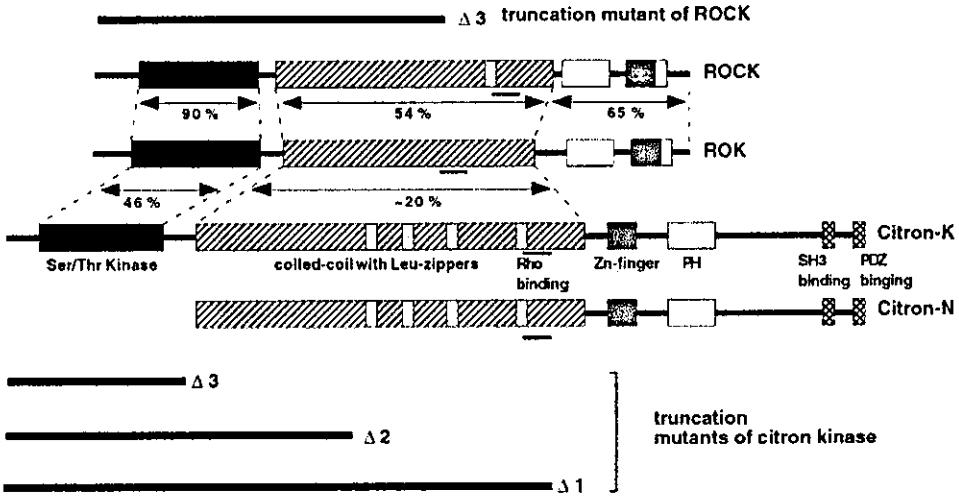

Figure 1. Schematic diagram of citron kinase, ROK and ROCK and their truncation mutants. Modified from Figure 1 of Madaule *et al.* (1998) with permission.

kinase mutants inhibits cytokinesis, suggesting that it may be a target of RhoA in cytokinesis (Madaule *et al.*, 1998). The involvement of citron kinase in cytokinesis is also supported by the phenotype of mice that are deficient of citron kinase (Di Cunto *et al.*, 2000). Mice lacking citron kinase showed severe ataxia and epilepsy and died within the 3 weeks after birth. Abnormal cytokinesis and massive apoptosis in certain neuronal precursors are suggested to be probable causes of defective neurogenesis. Although those results suggest that citron kinase is involved in cytokinesis, the mechanism is not clear. No physiological substrate of the kinase has been identified, and this is essential to elucidate the actions of citron kinase in cytokinesis and other biological processes.

We found that citron kinase phosphorylated regulatory myosin light chain (MLC) of myosin II at both Ser-19 and Thr-18 in vitro. In vivo, citron kinase generated di-phosphorylated MLC when its kinase domain was expressed in cultured cells. Our results suggest citron kinase may be involved in the regulation of contractile activity and/or organization of cleavage furrows by regulating MLC diphosphorylation.

MATERIALS AND METHODS

Expression Vectors, Proteins, Reagents, and Antibodies

Mammalian expression vectors of pCAG-myc-citron kinase (full-length, Δ1, Δ2, and Δ3 deletion mutants and kinase-deficient mutants), as well as pEGFPC1-citron kinase and pCAG-myc-ROCK1 Δ3 deletion mutant, were described previously (Ishizaki *et al.*, 1997; Madaule *et al.*, 1998; Eda *et al.*, 2001), and the domain structure of citron kinase and its mutants are depicted in Figure 1. Although the Δ3 mutant of citron kinase consists of the kinase domain of citron kinase alone, the Δ2 mutant contains both the kinase domain and half of the coiled-coil domain, which is structurally equivalent to the Δ3 deletion mutant of ROCK. The Δ1 mutant of citron kinase has further extension at the C terminus containing the Rho-binding domain (see Madaule *et al.*, 1998 for detail). A bacterial expression vector of pGEX-2T V14RhoA was kindly provided by Dr. A. Hall.

His-tagged, full-length citron kinase was expressed in Baculovirus using the Bac-to-Bac system (Invitrogen, Carlsbad, CA). Full-length citron kinase was cloned at *Sal*I (5′ end) and *Xho*I (3′ end) of the pENTR A1 Gateway vector and then transferred to the pDEST10 vector (N-terminal His fusion vector). Virus production and citron kinase expression were followed according to the manufacturer's instruction manual. Full-length citron kinase was purified by two steps of sequential affinity column chromatography. Cell lysates of infected Sf9 cells (~2 × 10^8) were first bound to a Nickel column and eluted with a linear gradient (50–200 mM) of imidazole. Citron kinase eluted around 80 mM was bound to a GST RhoA column and eluted as a complex of GST-RhoA-citron kinase. About 1–2 μg of purified kinase was prepared.

Nonmuscle myosin II was purified from bovine lung as described (Sellers, 1991). Light chains of myosin II were purified as described (Perrie and Perry, 1970). MLCK was purified from chick gizzard as described (Adelstein and Klee, 1981a). MBS of myosin phosphatase was purified from chick gizzard according to Alessi *et al.* (1992). Calmodulin was purchased from Sigma (St. Louis, MO). A specific inhibitor of ROCK, Y-27632, was kindly provided by Yoshitomi Pharmaceutical Industries, Ltd. (Oosaka, Japan).

An antimyc polyclonal antibody and an antimyc mAb (9E10) were purchased from Santa Cruz Biotechnology (Santa Cruz, CA) and Covance (Denver, PA), respectively. Chick antimyc polyclonal antibody was purchased from Aves Lab, Inc. (Tigard, OR). Monoclonal and polyclonal antibodies against Ser 19-phosphorylated MLC were described previously (Sakurada *et al.*, 1994; Matsumura *et al.*, 1998). A polyclonal antibody against di-phosphorylated (phosphorylated at both Ser 19 and Thr 18) MLC was described previously (Sakurada *et al.*, 1998).

Cell Culture, DNA Transfection, and Immunoprecipitation

PtK2 cells were maintained in a 1:1 mixture of DME and F12 medium containing 10% fetal calf serum. BHK, NRK, CHO, and COS7 cells were maintained in DME medium containing 10% fetal calf serum. Transfection was performed using a GeneJuice (Novagene, Madison, WI) or Lipofectamine (Invitrogen, Carlsbad, CA) transfection reagent.

For immunoprecipitation of exogenously expressed citron kinase or ROCK, COS7 cells were transfected with the myc-tagged constructs of citron kinase or ROCK according to manufacturer's instructions. After a 24-h incubation, transfected cells were lysed in an immunoprecipitation buffer containing 30 mM Tris-HCl (pH 7.5), 100 mM NaCl, 5 mM $MgCl_2$, 50 mM sodium pyrophosphate, 1 mM EGTA, 1 mM EDTA, 20 mM beta-glycerophosphate, 1 mM sodium vanadate, 10 mM NaF, 1% Triton X-100, 1 mM DTT, 1 mM PMSF,